

Wireless-Powered Device-to-Device-Assisted Offloading in Cellular Networks

Bodong Shang, *Student Member, IEEE*, Liqiang Zhao, *Member, IEEE*,
Kwang-Cheng Chen, *Fellow, IEEE*, and Xiaoli Chu, *Senior Member, IEEE*

Abstract—Offloading cellular traffic to device-to-device (D2D) communications has been proposed to improve the network capacity and to alleviate the traffic burden on base stations (BSs). However, as mobile devices are powered by limited battery energy, there is no obligation for D2D transmitters (D2D-Txs) to offload cellular traffic through D2D content sharing. In this paper, we model and analyze the wireless-powered D2D-assisted offloading (WPDO) in cellular networks, where the D2D-Txs can harvest radio frequency (RF) energy from nearby BSs and utilize the harvested energy to share popular contents with nearby user equipments (UEs). Stochastic geometry is used to characterize the intrinsic relationship between the wireless power transfer (WPT) and the information transmission. Based on the proposed model, we derive the average transmit power at D2D-Tx, the expected minimum transmit power at BS, the D2D outage probability, and the cellular downlink outage probability. We also investigate the energy efficiency of the WPDO network from a system-level perspective. Simulation and numerical results show that the energy efficiency of the WPDO network can be maximized by optimizing the fraction of time allocated for WPT and it can be further improved by using massive antenna arrays at each BS and by sharing more popular contents between devices.

Index Terms—D2D communications, energy efficiency, traffic offloading, cellular networks, wireless power transfer.

I. INTRODUCTION

WITH the upsurge of mobile data traffic and the explosively increase of mobile devices, cellular networks are facing technical challenges in supporting enormous data flows, high data rate, and large system capacity. In high user density areas, the base stations (BSs) are suffering heavy load burdens. To address the above issues, device-to-device (D2D) communications have been proposed to improve the network

capacity and to alleviate the traffic burden on cellular networks by exploiting the physical proximity of mobile devices [2]. In D2D communications, nearby devices can communicate with each other directly without using conventional cellular links, enjoying an improved received signal strength due to the short link distance.

However, as mobile devices are powered by limited battery energy, in general there is no obligation for mobile devices to participate in cellular traffic offloading or D2D content sharing [3]. Dedicated wireless power transfer (WPT) through electromagnetic radiation has emerged as a cost-effective technique to enable on-demand energy supplies and uninterrupted operations [4], [5]. The radio frequency (RF) signal emitted by dedicated energy sources, such as the hybrid access point (HAP) [6], which can provide both the energy and information transmission to/from user equipment (UE), can be used to supply energy over a long distance to UE.

In this paper, we incorporate WPT into D2D communications to facilitate D2D-assisted cellular traffic offloading. Considering the increasing power consumption of wireless networks [7], we propose an energy efficient wireless-powered D2D-assisted offloading (WPDO) network, where the D2D transmitters (D2D-Txs) scavenge RF energy from the nearest BS by pointing beams towards them as well as the ambient RF energy emitted by other BSs, and utilize the harvested energy to share popular contents with content requesters located in the D2D-Txs' offloading regions. In the offloading regions, the quality-of-service (QoS) requirements of the offloaded UEs (i.e., the D2D receivers) can be guaranteed. By leveraging tools from stochastic geometry, we evaluate the energy efficiency of the WPDO network and provide insights into the network design from a system-level perspective.

A. Related Works

The existing work on cellular traffic offloading can be categorized as follows: traffic offloading through small cells [8], traffic offloading through WiFi networks [9], traffic offloading through D2D communications [10]–[12]. Although offloading traffic from macro cells to small cells provides a convenient way to mitigate cellular network congestions, the decreasing coverage probability due to inter-cell interference [13] and the expensive operating cost for backhaul links hinder the dense deployment of small cells [14]. Different from cellular technologies, WiFi networks provide higher data rates by exploiting wider unlicensed frequency bandwidths and higher-order modulations [15]. However, in WiFi-assisted offloading

Manuscript received March 6, 2018; revised April 23, 2018; accepted May 14, 2018. Date of publication May XX, 2018; date of current version XX XX, 2018. This work was supported in part by the National Natural Science Foundation of China under Grant 61771358, in part by the Intergovernmental International Cooperation on Science and Technology Innovation under Grant 2016YFE0122900, in part by the China Postdoctoral Science Foundation under Grant 2017M613074, in part by the Fundamental Research Funds for the Central Universities under Grant JB170102, in part by the 111 Project under Grant B08038, and in part by the starting fund for K.-C. Chen at the University of South Florida. This paper appeared in part at the IEEE Global Communications Conference (GLOBECOM) 2017, Singapore, Dec 2017 [1]. The associate editor coordinating the review of this paper and approving it for publication was E. Ayanoglu. (*Corresponding author: Liqiang Zhao*)

Bodong Shang and Liqiang Zhao are with the State Key Lab. of ISN, Xidian University, China (emails:bdshang@hotmail.com, lqzhao@mail.xidian.edu.cn).

Kwang-Cheng Chen is with the Department of Electrical Engineering, University of South Florida, USA (email:kwangcheng@usf.edu).

Xiaoli Chu is with the Department of Electronic and Electrical Engineering, University of Sheffield, UK, (email:x.chu@sheffield.ac.uk).

Digital Object Identifier XX.XXXX/TGCN.2018.XXXXXXX.

networks, the UE mobility management and the network coverage are limited [9]. In D2D-assisted offloading networks, popular contents can be shared directly among mobile devices as an economical way to alleviate the traffic burden on cellular BSs [10], [11], however, at the cost of increased power/energy consumption at D2D-Txs. In [3], [16], [17], incentive schemes were investigated to stimulate UEs to participate in D2D communications. In [12], [18], the social interactions among UEs, either in real life or in social networks, were exploited in the design of D2D communications.

With the development of the wireless charging techniques [19], it has been proposed to harvest RF energy for powering information transmission in cellular networks [20], [21], as well as in D2D communications [22]–[24]. In [24], energy harvesting D2D communications were designed to maximize the sum-rate for D2D links. However, it has been shown that, the energy harvested from ambient RF signals can only power small sensors with sporadic activities [25], while supplying stable and fully controllable power for D2D communications would require dedicated WPT [5]. In [26], unmanned aerial vehicles were used as dedicated energy sources to provide WPT to UEs, where the resource allocation was optimized to maximize the average throughput. In [27], the sum rate of wireless-powered D2D links was maximized by jointly optimizing beamforming and resource allocation. Note that most of the above works focused on a single cell and ignored the interference between cellular and D2D links, which may significantly affect the performance of both the cellular network and the D2D links. In addition, none of the existing works has studied the energy efficiency of wireless-powered D2D assisted offloading networks while considering the UEs' QoS requirements.

B. Paper Contributions

In our proposed WPT enabled D2D-assisted offloading networks, a communication time slot is divided into two sub-slots. In the first sub-slot, each BS with a large antenna array wirelessly charges the D2D-Txs located in its coverage area by direct beamforming. In the second sub-slot, D2D-Txs utilize the harvested energy to broadcast popular contents to nearby mobile content requesters, and BSs perform downlink transmissions to their scheduled cellular UEs. We consider the underlay mode of D2D communications and thus the mutual interference between cellular and D2D links.

The main contributions of the paper are summarized as follows:

- We develop a tractable analytical model for the WPDO network. Using stochastic geometry, we derive the expressions for the average transmit power of a typical D2D-Tx and the expected minimum transmit power at a typical BS while meeting cellular UEs data rate requirements, and investigate the relationship between the D2D-Tx average transmit power and the density of D2D-Txs as well as the size of antenna arrays at BSs.
- Based on the D2D-Tx average transmit power, we derive the outage probabilities of D2D and cellular UEs, respectively. The D2D outage probability is analyzed as

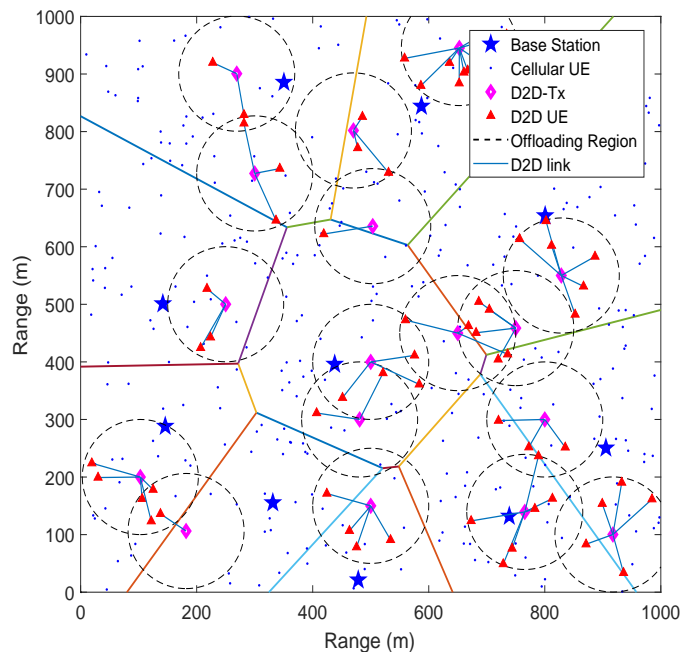


Fig 1: Wireless-powered D2D-assisted offloading (WPDO) in the cellular downlink networks, where D2D-Txs scavenge RF energy from the nearest BS by pointing beams towards them as well as the ambient RF energy emitted by other BSs, and utilize the harvested energy to share popular contents with content requesters located in the D2D-Txs' offloading regions with the radius \mathcal{R}_D , where $\mathbb{P}_{con} = 0.3$.

a function of the time allocation factor (i.e., the fraction of time allocated for WPT) and the D2D UE data rate requirement.

- We define and maximize the network energy efficiency for WPDO by optimizing the time allocation factor, and provide insights into the design of an energy-efficient WPDO network, with respect to the time allocation factor, the popularity of contents shared via D2D, and the size of BS antenna arrays.

C. Paper Organization

The remainder of this paper is organized as follows. In Section II, the system model is presented. Section III derives the average transmit power at a typical D2D-Tx and the BS expected minimum transmit power. Section IV gives the analytical expressions of the outage probabilities for D2D UE and cellular UE, respectively. Section V defines and optimizes the WPDO network energy efficiency. Simulation and numerical results are presented in Section VI. Finally, conclusions are drawn in Section VII.

Notation: $\mathbb{E}\{x\}$ denotes the expectation of variable x . $\mathbb{P}\{A\}$ denotes the probability that event A happens. Finally, y^* denotes the optimal value of y .

II. SYSTEM MODEL

A. Network Topology

We consider the cellular downlink underlaid with D2D communications, where the D2D-Txs can broadcast popular contents to other UEs in their proximity as shown in Fig. 1. The BSs are distributed following a homogeneous Poisson Point Process (PPP) on the entire network

plane \mathbb{R}^2 with the density λ_B and are denoted by the set $\Phi_B = \{b_j, j = 0, 1, 2, \dots\}$. Each BS has a maximum allowable transmit power P_m and is equipped with N_t antennas. The cell area of the j^{th} BS b_j is given by $V_j = \{x \in \mathbb{R}^2 \mid \|x - b_j\| \leq \|x - b_n\|, b_n \in \Phi_B \setminus b_j\}$, where $\|a - b\|$ represents the Euclidean distance between a and b in the plane \mathbb{R}^2 . Since there is no interference concern in the downlink wireless power transfer phase, each BS can adopt the simple maximal ratio transmission (MRT) beamforming to maximize the wirelessly transferred power to the D2D-Txs in its cell area. Most of the other beamforming methods, such as zero-forcing (ZF) beamforming, are designed to mitigate interference at the cost of reduced radiated power gain [28]. D2D-Txs are distributed following an independent homogeneous PPP denoted by Φ_D with the density λ_D . UEs¹ are spatially scattered in \mathbb{R}^2 following another independent PPP denoted by the set Φ_U with the density λ_U , which can be classified into cellular UEs (served by BSs) and D2D UEs (served by D2D links). Each UE is assumed to be equipped with a single antenna.

B. UE Association

In our system model, each cellular UE connects to the closest BS. Each D2D-Tx centers at its offloading region with the radius \mathcal{R}_D , which is set to guarantee the D2D data rate requirement in the offloading region (see Section V). The data rate requirements of cellular UEs and D2D UEs are denoted by R_c and R_d (Mbps), respectively. We define the content popularity of a content available at a D2D-Tx as the probability \mathbb{P}_{con} that the content is requested by at least one UE. The content popularity can be obtained by the keywords feature extraction method [29] or the machine learning method [30] according to the UEs' download history. If a content requesting UE is located in the offloading region of a D2D-Tx containing the requested contents, then the UE will be informed by its serving BS to connect with the D2D-Tx.

C. Channel Model

The downlink bandwidth is B MHz, which is shared between cellular downlink and D2D communications. Each BS performs adaptive power control according to the channel state information (CSI) obtained from UE feedback [31] and adopts MRT beamforming to transmit the information to cellular UEs. According to Shannon's theorem, the transmit power $P_{i,j}^B$ of BS b_j for cellular UE $u_{i,j}^c$ (i.e., the i^{th} cellular UE in the j^{th} cell) to achieve the required data rate R_c can be obtained by solving the following equation:

$$R_c = \frac{B}{N_j^c} \log_2 \left(1 + \text{SINR} \left(u_{i,j}^c \right) \right), \quad (1)$$

where

$$\text{SINR} \left(u_{i,j}^c \right) = \frac{P_{i,j}^B \left\| \mathbf{h}_{b_j u_{i,j}^c} \right\|^2 H_\alpha \left\| b_j - u_{i,j}^c \right\|^{-\alpha}}{I_{u_{i,j}^c}^C + I_{u_{i,j}^c}^D + \sigma^2} \quad (2)$$

¹In this paper, UEs refer to the information receivers which includes the cellular UEs and the D2D UEs (i.e., D2D receivers).

Table I: Main variables used throughout the paper

Notation	Description
Φ_B, Φ_D, Φ_U	Sets of cellular BSs, D2D-Txs and UEs
$\lambda_B, \lambda_D, \lambda_U$	Densities of cellular BSs, D2D-Txs and UEs per square meter
B	Bandwidth of cellular network and D2D communications
b_j	The j^{th} BS in the network
N_t	The number of antennas at a cellular BS
R_c, R_d	Required data rates of cellular and D2D UEs
P_m	Maximum allowable transmit power of BSs
$u_{i,j}^c$	The i^{th} cellular UE in j^{th} cell of BS b_j
$\Phi_{u,j}^c$	Set of cellular UEs in the cell of BS b_j
N_j^c	The number of cellular UEs in the cell of b_j
T	The duration of a communication time slot
θ	Time allocation factor for WPT
$d_{k,j}$	The k^{th} D2D-Tx in the cell of BS b_j
$u_{i,k,j}^d$	The i^{th} D2D UE connecting with $d_{k,j}$
P_d	Average transmit power of a typical D2D-Tx
\mathbb{P}_{con}	Content popularity of the shared contents
P_c^{out}, P_d^{out}	Outage probability of cellular and D2D UEs
ε	Maximum acceptable outage probability

where N_j^c denotes the total number of cellular UEs served by BS b_j , $\mathbf{h}_{b_j u_{i,j}^c} \in C^{1 \times N_t}$ is the small-scale fading channel vector², H_α is a frequency dependent constant value [13], which is commonly set as $\left(\frac{c}{4\pi f_\alpha} \right)^2$ with $c = 3 \times 10^8$ m/s and the carrier frequency f_α , α is the path loss exponent, $I_{u_{i,j}^c}^C$ and $I_{u_{i,j}^c}^D$ denote the interference power from interfering BSs and from D2D-Txs to $u_{i,j}^c$, respectively, and σ^2 is the additive noise. Specifically, we have

$$I_{u_{i,j}^c}^C = \sum_{b_n \in \Phi_B \setminus b_j} P_{i,n}^B \left| \mathbf{h}_{b_n u_{i,j}^c} \frac{\mathbf{g}_{b_n u_{i,n}^c}^H}{\left\| \mathbf{g}_{b_n u_{i,n}^c} \right\|} \right|^2 H_\alpha \left\| b_n - u_{i,j}^c \right\|^{-\alpha}, \quad (3)$$

and

$$I_{u_{i,j}^c}^D = \sum_{d_k \in \Phi_D} P_{d,k} h_{d_k u_{i,j}^c} H_\alpha \left\| d_k - u_{i,j}^c \right\|^{-\alpha} \quad (4)$$

where $\mathbf{h}_{b_n u_{i,j}^c} \in C^{1 \times N_t}$ is the interfering small-scale fading channel vector, and $\frac{\mathbf{g}_{b_n u_{i,n}^c}^H}{\left\| \mathbf{g}_{b_n u_{i,n}^c} \right\|}$ is the MRT beamforming vector of BS b_n , where $\mathbf{g}_{b_n u_{i,n}^c} \in C^{1 \times N_t}$ is the small-scale fading channel vector from BS b_n to its associated UE $u_{i,n}^c$. According to eq.(3) of [32] and Proposition 1 of [33], $\mathbf{h}_{b_n u_{i,j}^c} \frac{\mathbf{g}_{b_n u_{i,n}^c}^H}{\left\| \mathbf{g}_{b_n u_{i,n}^c} \right\|}$ is a zero-mean complex Gaussian variable.

D. Wireless Power Transfer

Since we assume that each D2D-Tx is equipped with one antenna either for energy harvesting or for information transmission and to ease the energy consumption burden on D2D-Txs in D2D-assisted offloading, we employ the harvest-then-transmit protocol [21], where the D2D-Tx first harvests

²With a slight abuse of notation we will use \mathbf{h}_{xy} to denote the small-scale fading channel vector from x to y , where the channels are assumed to experience Rayleigh fading such that $\|\mathbf{h}_{xy}\|^2 \sim \text{Gamma}(N_t, 1)$.

the wireless energy from both the directed power transferred by its nearest BS and the ambient power radiated by other BSs, and then utilizes the harvested energy to send data to D2D UEs. Note that simultaneous energy harvesting and information transmission at the D2D-Tx would require multiple antennas and an integrated circuit architecture, resulting in additional costs and increased complexities in circuit design and antenna array configuration at the UEs [34]. Let T denote the duration of a communication time slot, which is divided into two sub-slots of duration θT and $(1 - \theta) T$, respectively, where θ ($0 \leq \theta \leq 1$) is the time allocation factor. The θT sub-slot is allocated for WPT and the $(1 - \theta) T$ sub-slot is for information transmission. In WPT, the D2D-Txs in a cell take turns to harvest RF energy from the nearest BS by direct beamforming as well as the ambient RF energy from other BSs for a time duration of $\frac{\theta T}{n_d}$, where n_d denotes the number of D2D-Txs in a cell and $\mathbb{E}\{n_d\} = \frac{\lambda_D}{\lambda_B}$. Therefore, the instantaneous received power $P_{d_{k,j}}^{r, \frac{1}{n_d} \theta T}$ at the k^{th} D2D-Tx $d_{k,j}$ in the j^{th} cell during the allocated time $\frac{\theta T}{n_d}$ is expressed as

$$\begin{aligned} P_{d_{k,j}}^{r, \frac{1}{n_d} \theta T} &= P_{S_{b_j}}^{r, \frac{1}{n_d} \theta T} + P_{S_{\Phi_B \setminus b_j}}^{r, \frac{1}{n_d} \theta T} \\ &= P_m \|\mathbf{h}_{b_j d_{k,j}}\|^2 H_\beta (\max\{\|b_j - d_{k,j}\|, v_1\})^{-\beta} \\ &\quad + \sum_{b_n \in \Phi_B \setminus b_j} \frac{P_m \left| \mathbf{h}_{b_n d_{k,j}} \frac{\mathbf{g}_{b_n d_{l,n}}^H}{\|\mathbf{g}_{b_n d_{l,n}}\|} \right|^2 H_\beta}{(\max\{\|b_n - d_{l,n}\|, v_1\})^\beta} \end{aligned} \quad (5)$$

where β is the path loss exponent for a WPT link, and v_1 ($v_1 \geq 1$) is used to avoid singularity at zero distance and to ensure the finite moments of the direct and the ambient RF signals. It is worth noting that the carrier frequencies of WPT and information transmission are different. H_β is a frequency dependent constant value of a WPT link.

In addition, during the remaining time of $\frac{(n_d-1)\theta T}{n_d}$, the typical D2D-Tx harvests the ambient RF energy emitted by all BSs in the network. Thus, the instantaneous received power $P_{d_{k,j}}^{r, \frac{n_d-1}{n_d} \theta T}$ at D2D-Tx $d_{k,j}$ during $\frac{(n_d-1)\theta T}{n_d}$ is given by

$$\begin{aligned} P_{d_{k,j}}^{r, \frac{n_d-1}{n_d} \theta T} &= P_{S_{\Phi_B}}^{r, \frac{n_d-1}{n_d} \theta T} \\ &= \sum_{b_n \in \Phi_B, l \neq k} \frac{P_m \left| \mathbf{h}_{b_n d_{k,j}} \frac{\mathbf{g}_{b_n d_{l,n}}^H}{\|\mathbf{g}_{b_n d_{l,n}}\|} \right|^2 H_\beta}{(\max\{\|b_n - d_{l,n}\|, v_1\})^\beta}. \end{aligned} \quad (6)$$

We assume that each D2D-Tx has a rechargeable battery with a sufficiently large storage such that enough harvested energy can be stored at D2D-Txs for supporting stable transmit power. The randomness of the instantaneous received power at a D2D-Tx can be averaged out, and a fixed transmit power up to \bar{P}_d can be provided [20], [35]. Note that if a D2D-Tx has a small battery storage, the battery may be saturated and the additionally arriving energy will be discarded without being utilized for data transmission [36].

In addition, \bar{P}_d is expressed as follows

$$\bar{P}_d = \eta \frac{1}{(1-\theta)T} \mathbb{E}\{E_{d_{k,j}}^{r, \theta T}\} \quad (7)$$

where η ($0 < \eta < 1$) is the RF-to-DC conversion efficiency [37] and $\mathbb{E}\{E_{d_{k,j}}^{r, \theta T}\}$ is the expectation of the total received RF energy at a typical D2D-Tx $d_{k,j}$ during θT , and we have

$$E_{d_{k,j}}^{r, \theta T} = \frac{\theta T}{n_d} P_{d_{k,j}}^{r, \frac{1}{n_d} \theta T} + \frac{(n_d - 1) \theta T}{n_d} P_{d_{k,j}}^{r, \frac{n_d-1}{n_d} \theta T}. \quad (8)$$

To achieve a reliable transmit power and to avoid the interruptions caused by energy shortage at a D2D-Tx, we assume that the energy consumed for information transmission of a D2D-Tx should not exceed the harvested energy [35].

E. D2D Information Transmission

In D2D information transmission, the signal-to-interference-plus-noise (SINR) ratio at the i^{th} D2D UE $u_{i,k,j}^d$ connecting with $d_{k,j}$ is given by

$$\text{SINR}(u_{i,k,j}^d) = \frac{\bar{P}_d h_{d_{k,j} u_{i,k,j}^d} H_\alpha \|d_{k,j} - u_{i,k,j}^d\|^{-\alpha}}{I_{u_{i,k,j}^d}^C + I_{u_{i,k,j}^d}^D + \sigma^2}, \quad (9)$$

where

$$I_{u_{i,k,j}^d}^C = \sum_{b_n \in \Phi_B} P_{i,n}^B \left| \mathbf{h}_{b_n u_{i,k,j}^d} \frac{\mathbf{g}_{b_n u_{i,n}^c}}{\|\mathbf{g}_{b_n u_{i,n}^c}\|} \right|^2 \frac{H_\alpha}{\|b_n - u_{i,k,j}^d\|^\alpha}, \quad (10)$$

$$I_{u_{i,k,j}^d}^D = \sum_{d_n \in \Phi_D \setminus d_{k,j}} \bar{P}_d h_{d_n u_{i,k,j}^d} H_\alpha \|d_n - u_{i,k,j}^d\|^{-\alpha}, \quad (11)$$

where $h_{d_{k,j} u_{i,k,j}^d} \sim \exp(1)$ is the channel power gain, $I_{u_{i,k,j}^d}^C$ denotes the interference power from cellular transmissions, and $I_{u_{i,k,j}^d}^D$ denotes the interference power from D2D communications.

A D2D outage occurs when the data rate of a D2D link with a distance \mathcal{R}_D falls below the D2D data rate requirement R_d during a communication time slot T . The outage probability of D2D communications is given by

$$\begin{aligned} P_d^{\text{out}} &= 1 - \mathbb{P} \left\{ \frac{(1-\theta)T}{T} B \right. \\ &\quad \left. \cdot \log_2 \left(1 + \frac{\bar{P}_d h_{d_{k,j} u_{i,k,j}^d} H_\alpha \mathcal{R}_D^{-\alpha}}{I_{u_{i,k,j}^d}^C + I_{u_{i,k,j}^d}^D + \sigma^2} \right) \geq R_d \right\}. \end{aligned} \quad (12)$$

The D2D outage probability needs to be kept below a certain threshold ε (i.e., $P_d^{\text{out}} \leq \varepsilon$).

III. SYSTEM-LEVEL PERFORMANCE EVALUATION

In this section, to evaluate the WPT efficiency and the performance of subsequent D2D information transmission, we characterize the average transmit power of a typical D2D-Tx and the BS expected minimum transmit power based on a system-level analysis.

A. Average Transmit Power Of D2D-Tx

Proposition 1. *In the WPDO network, given the BS density λ_B , the BS antenna array size N_t , the transmit power P_m in*

WPT, and the density of D2D-Txs λ_D , the average transmit power at a typical D2D-Tx is given by

$$\begin{aligned} \overline{P_d} = & \frac{\eta\theta P_m H_\beta \lambda_B}{(1-\theta)\lambda_D} \left[\frac{\Gamma\left(\frac{2-\beta}{2}, \pi\lambda_B v_1^2\right)}{N_t^{-1}(\pi\lambda_B)^{-\frac{\beta}{2}}} + \frac{2\Gamma\left(\frac{4-\beta}{2}\right)}{\beta-2} \right. \\ & \left. \cdot \frac{(\pi\lambda_B)^{\frac{\beta}{2}}}{e^{\pi\lambda_B v_1^2}} + \frac{\frac{\pi\lambda_B v_1^2 \beta}{\beta-2} - 1 + N_t}{v_1^\beta (1 - e^{-\pi\lambda_B v_1^2})^{-1}} + \frac{\left(1 - \frac{\lambda_B}{\lambda_D}\right) \lambda_D \pi \beta}{v_1^{\beta-2} (\beta-2)} \right] \end{aligned} \quad (13)$$

where $\Gamma(s, x) = \int_0^\infty t^{s-1} e^{-t} dt$ is the incomplete Gamma function, $\Gamma(x) = \int_0^\infty t^{x-1} e^{-t} dt$ is the Gamma function.

Proof: Please refer to Appendix A for the proof. ■

From Proposition 1, we can see that the average transmit power of a typical D2D-Tx increases with the time allocation factor θ , the BS density λ_B and the BS antenna array size N_t . Next, we present the average transmit power of a typical D2D-Tx for the special case of $\lambda_D = \lambda_B$, i.e., each BS wirelessly powers one D2D-Tx during θT .

Corollary 1. With $\lambda_D = \lambda_B$, the average transmit power of a typical D2D-Tx reduces to

$$\begin{aligned} \overline{P_d} = & \frac{\eta\theta P_m H_\beta}{1-\theta} \left[\frac{\Gamma\left(\frac{2-\beta}{2}, \pi\lambda_B v_1^2\right)}{N_t^{-1}(\pi\lambda_B)^{-\frac{\beta}{2}}} + \frac{2\Gamma\left(\frac{4-\beta}{2}\right)}{\beta-2} \right. \\ & \left. \cdot \frac{(\pi\lambda_B)^{\frac{\beta}{2}}}{e^{\pi\lambda_B v_1^2}} + \frac{\frac{\pi\lambda_B v_1^2 \beta}{\beta-2} - 1 + N_t}{v_1^\beta (1 - e^{-\pi\lambda_B v_1^2})^{-1}} \right]. \end{aligned} \quad (14)$$

B. BS Expected Minimum Transmit Power

In the following proposition, we characterize the expected minimum transmit power of a typical BS in the WPDO network, subject to the number of cellular UEs in its cell.

Proposition 2. In the WPDO network, given the BS density λ_B , the BS antenna array size N_t , and the cellular UE data rate requirement R_c , the expected minimum transmit power of BS b_j conditioned on the number of cellular UEs N_j^c in its cell is given by

$$\begin{aligned} \mathbb{E}\{P_{i,j}^B | N_j^c\} = & \frac{\left(2^{\frac{N_j^c R_c}{(1-\theta)B}} - 1\right) 2P_m H_\alpha}{N_t (\alpha - 2)} + \frac{2^{\frac{N_j^c R_c}{(1-\theta)B}} - 1}{N_t} \\ & \cdot \left\{ \left[\frac{\pi\lambda_D \overline{P_d} H_\alpha \alpha}{v_2^{\alpha-2} (\alpha-2)} + \sigma^2 \right] \frac{\Gamma\left(\frac{\alpha}{2} + 1\right)}{(\pi\lambda_B)^{\frac{\alpha}{2}}} + \right\}. \end{aligned} \quad (15)$$

where $\overline{P_d}$ is given in Proposition 1.

Proof: Please refer to Appendix B for the proof. ■

Recall that a cellular UE can be offloaded to D2D link if the following two conditions are both satisfied. First, the cellular UE locates within the offloading region of a D2D-Tx. Second, the UE's requested contents are available at that D2D-Tx.

Accordingly, we give the following Lemma to calculate the density of residual cellular UEs that are unable to be offloaded to D2D links in the WPDO network.

Lemma 1. In the WPDO network, given the BS density λ_B , the offloading radius \mathcal{R}_D of D2D-Txs, and the content

popularity \mathbb{P}_{con} , the density of residual cellular UEs λ_U^c is given by [16]

$$\lambda_U^c = e^{-\mathbb{P}_{con} \pi \lambda_D \mathcal{R}_D^2} \lambda_U. \quad (16)$$

Proof: Please refer to Appendix B in [16]. ■

Since the spatial distribution of cellular UEs follows a homogeneous PPP in plane \mathbb{R}^2 , the probability mass function (PMF) for the number of cellular UEs N_j^c can be approximately given by [38]

$$g_{N_j^c}(n) = \frac{\left(\frac{\lambda_U^c}{\lambda_B}\right)^n}{n!} \exp\left(-\frac{\lambda_U^c}{\lambda_B}\right). \quad (17)$$

Therefore, we have the following proposition on the expected minimum transmit power of a typical BS in the WPDO network.

Proposition 3. In the WPDO network, given the BS density λ_B , the BS antenna array size N_t , and the cellular data rate requirement R_c , the expectation of the minimum transmit power of BS b_j is given by

$$\begin{aligned} \mathbb{E}\{P_j^B\} = & \frac{\exp\left\{\left[2^{\frac{R_c}{(1-\theta)B}} - 1\right] \frac{\lambda_U^c}{\lambda_B}\right\} - 1}{N_t} \\ & \cdot \left\{ \left[\frac{\pi\lambda_D \overline{P_d} H_\alpha \alpha}{v_2^{\alpha-2} (\alpha-2)} + \sigma^2 \right] \frac{\Gamma\left(\frac{\alpha}{2} + 1\right)}{(\pi\lambda_B)^{\frac{\alpha}{2}}} + \frac{2P_m H_\alpha}{\alpha - 2} \right\} \end{aligned} \quad (18)$$

where λ_U^c is given in Lemma 1.

Proof: Based on (15) and (17), we have

$$\begin{aligned} \mathbb{E}\{P_j^B\} &= \sum_{n=1}^{\infty} \mathbb{E}\{P_{i,j}^B | N_j^c\} g_{N_j^c}(n) \\ &= \Psi \sum_{n=1}^{\infty} \left(2^{\frac{n R_c}{(1-\theta)B}} - 1\right) \frac{\left(\frac{\lambda_U^c}{\lambda_B}\right)^n}{n!} \exp\left(-\frac{\lambda_U^c}{\lambda_B}\right) \\ &= \Psi e^{-\frac{\lambda_U^c}{\lambda_B}} \left[\sum_{n=0}^{\infty} \frac{\left(2^{\frac{n R_c}{(1-\theta)B}} \cdot \frac{\lambda_U^c}{\lambda_B}\right)^n}{n!} - \sum_{n=0}^{\infty} \frac{\left(\frac{\lambda_U^c}{\lambda_B}\right)^n}{n!} \right] \\ &= \Psi \left\{ e^{\left[2^{\frac{R_c}{(1-\theta)B}} - 1\right] \frac{\lambda_U^c}{\lambda_B}} - 1 \right\} \end{aligned} \quad (19)$$

where

$$\Psi = \left[\frac{\pi\lambda_D \overline{P_d} H_\alpha \alpha}{v_2^{\alpha-2} (\alpha-2)} + \sigma^2 \right] \frac{\Gamma\left(\frac{\alpha}{2} + 1\right)}{N_t (\pi\lambda_B)^{\frac{\alpha}{2}}} + \frac{2P_m H_\alpha}{N_t (\alpha - 2)}. \quad (20)$$

Then we have the result in (18). ■

IV. OUTAGE PROBABILITY

In this section, we derive the outage probability of information transmission for D2D and cellular UEs in the WPDO network, which will be used for the evaluation of network energy efficiency in Section V.

A. Outage Probability Of A D2D Link

Following (12), the outage probability of a D2D link can be rewritten as

$$P_d^{out} = 1 - \mathbb{P} \{ SINR(u_{i,k,j}^d) \geq \gamma_{th}(\theta) | \mathcal{R}_D \} \quad (21)$$

where the SINR threshold $\gamma_{th}(\theta)$ is given by

$$\gamma_{th}(\theta) = 2^{\frac{R_d}{(1-\theta)B}} - 1. \quad (22)$$

In the following Proposition, we obtain the outage probability P_d^{out} of a typical D2D UE.

Proposition 4. *In the WPDO network, given the time allocation factor θ and the D2D UE data rate requirement R_d , the outage probability of a typical D2D UE is given by*

$$P_d^{out} = 1 - \exp \left\{ -\frac{2\Lambda\pi^2(\psi(\theta, R_d))^{\frac{2}{\alpha}}}{\alpha \sin(\frac{2\pi}{\alpha})} - \sigma^2\psi(\theta, R_d) \right\}$$

$$\text{and } \psi(\theta, R_d) = \frac{\gamma_{th}(\theta)}{\overline{P}_d H_\alpha \mathcal{R}_D^{-\alpha}}, \gamma_{th}(\theta) = 2^{\frac{R_d}{(1-\theta)B}} - 1$$

$$\Lambda = \lambda_B (\mathbb{E} \{ P_j^B \})^{\frac{2}{\alpha}} + \lambda_D (\overline{P}_d)^{\frac{2}{\alpha}} \quad (23)$$

where \overline{P}_d is given in (13) and $\mathbb{E} \{ P_j^B \}$ is given in (18).

Proof: Please refer to Appendix C for the proof. ■

In (23), we can observe that P_d^{out} approaches to 1 when $\theta \rightarrow 0$ or $\theta \rightarrow 1$, which is in line with the intuition. More specifically, $\theta \rightarrow 0$ indicates that there is no time allocated for WPT, and thus $\overline{P}_d \approx 0$ and $P_d^{out} \rightarrow 1$. Besides, $\theta \rightarrow 1$ indicates that no time is allocated for information transmission, which pushes the SINR threshold $\gamma_{th}(\theta)$ to infinity, and thus $\psi(\theta, R_d) \rightarrow \infty$ and $P_d^{out} \rightarrow 1$.

B. Outage Probability Of A Cellular Downlink

We define the outage probability of a cellular UE as follows

$$P_c^{out} = \mathbb{P} \{ P_j^B > P_m \} \quad (24)$$

which is the probability that the BS's expected minimum transmit power exceeds the maximum allowable transmit power P_m for guaranteeing the cellular UE's required data rate R_c .

The outage probability of a typical cellular UE in the WPDO network is presented in the following proposition.

Proposition 5. *In the WPDO network, given the time allocation factor θ , the cellular UE data rate requirement R_c , and the D2D offloading radius \mathcal{R}_D , the outage probability of a typical cellular UE is given by*

$$P_c^{out} = \frac{\alpha \lambda_B \Gamma(\frac{N_t}{2})}{\Gamma(N_t) \exp(\frac{\lambda_U^c}{\lambda_B})} \sum_{n=1}^{\infty} \int_0^{\infty} \int_0^{\infty} \frac{\sin(t \sin(\frac{2\pi}{\alpha})) y}{n!}$$

$$\cdot \frac{\left(\frac{\lambda_U^c}{\lambda_B}\right)^n \left(\frac{t^{\frac{\alpha}{2}} P_m}{T(n) y^{\alpha} \xi^{\frac{\alpha}{2}}} + 1\right)^{-\frac{N_t}{2}} e^{-\pi \lambda_B y^2}}{\pi \lambda_B \zeta\left(-\left(\frac{t}{\xi}\right)^{\frac{\alpha}{2}}, y, P_m\right) + \frac{t}{\sin(\frac{2\pi}{\alpha})} - \sigma^2 \left(\frac{t}{\xi}\right)^{\frac{\alpha}{2}}} dt dy$$

$$\text{with } \xi = \frac{2\lambda_D (\overline{P}_d)^{\frac{2}{\alpha}} \pi^2}{\alpha \sin(\frac{2\pi}{\alpha})}, T(n) = 2^{\frac{R_c n}{(1-\theta)B}} - 1 \quad (25)$$

where \overline{P}_d is given in (13) and λ_U^c is given in (16).

Proof: Please refer to Appendix D for the proof. ■

The result in (25) involves two integrations and a summation of series which can be obtained by numerical calculations. We can observe from the expression in (25) that the outage probability of a typical cellular UE decreases with the increasing number of antennas used at each BS.

V. NETWORK ENERGY EFFICIENCY

The WPDO network energy efficiency (η_{EE}) is defined as the ratio of area spectral efficiency (ASE) to area power consumption (APC) as follows

$$\eta_{EE} = \frac{ASE}{APC} \quad (26)$$

where the ASE refers to the sum rate of both cellular and D2D UEs per unit area per Hz, while the APC is the total power consumption per unit area.

More specifically, we have

$$ASE = \frac{\lambda_B (1 - P_c^{out}) R_c + (\lambda_U - \lambda_U^c) (1 - P_d^{out}) R_d}{B} \quad (27)$$

where we assume that each BS is active and serves one cellular UE per channel, and the cellular UEs within the same cell are scheduled based on time-division multiple access (TDMA); P_c^{out} and P_d^{out} are the cellular and D2D outage probabilities given in (25) and (23), respectively; $\lambda_U - \lambda_U^c$ denotes the density of D2D UEs, while λ_U^c is given in (16).

The APC is given by

$$APC = (1 - \theta) \lambda_B \mathbb{E} \{ P_j^B \} + \theta \lambda_B P_m \quad (28)$$

where the APC includes the BS power consumptions for down-link information transmission and for WPT towards D2D-Txs, and $\mathbb{E} \{ P_j^B \}$ is given in (18).

Note that the time allocation factor θ should be carefully selected for achieving a high WPDO network energy efficiency. In the following, based on our analytical results from previous sections, we propose an algorithm to maximize the WPDO network energy efficiency while guaranteeing that the D2D outage probability is below a certain value ε , i.e., the maximum acceptable outage probability. Based on (23), letting $P_d^{out} = \varepsilon$ (as shown in (29) at the bottom of next page) and solving it for \mathcal{R}_D by numerical methods, we can obtain the D2D-Tx's offloading radius \mathcal{R}_D for a given θ . Based on \mathcal{R}_D , (13), (16), (18), (23) and (25-28), we can obtain the maximum WPDO network energy efficiency η_{EE}^* and can acquire the near-optimal time allocation factor θ^* by an exhaustive search. In Algorithm 1, we summarize the main steps of obtaining θ^* and η_{EE}^* , where the searching space is (0, 1) and the searching step size is ω .

Please note that in this paper, we focus on the modeling and analysis of an energy efficient WPDO network from a system-level perspective. The optimization algorithm design for obtaining the optimal value of θ is beyond the scope of this paper.

Next, we present the closed-form expression of the D2D-Tx's offloading radius \mathcal{R}_D for two special cases and provide insights into the design of energy-efficient WPDO networks.

Special case 1: For the path loss exponent $\alpha = 4$, \mathcal{R}_D in (29) becomes

$$\mathcal{R}_D = \left[\frac{\sqrt{\frac{\Lambda^2 \pi^4}{4} - 4\sigma^2 \ln(1-\varepsilon)} - \frac{\Lambda \pi^2}{2}}{2\sigma^2 \left(\frac{\gamma_{th}(\theta)}{P_d H_\alpha} \right)^{\frac{1}{2}}} \right]^{\frac{1}{2}} \quad (30)$$

where Λ and $\gamma_{th}(\theta)$ are given in (23).

Special case 2: For an interference limited network, i.e., $\sigma^2 \approx 0$, \mathcal{R}_D in (29) reduces to

$$\mathcal{R}_D = \frac{\sqrt{-\ln(1-\varepsilon)}}{\pi \sqrt{\frac{2\Lambda}{\alpha \sin\left(\frac{2\pi}{\alpha}\right)} \left(\frac{\gamma_{th}(\theta)}{P_d H_\alpha} \right)^{\frac{1}{\alpha}}}} \quad (31)$$

where Λ and $\gamma_{th}(\theta)$ are given in (23).

Remark: In (30) and (31), since $-\ln(1-\varepsilon)$ is a monotonically increasing function of ε ($0 < \varepsilon < 1$), the D2D-Tx offloading radius increases with the value of the maximum acceptable outage probability ε . In addition, we observe that $\mathcal{R}_D \approx 0$ when $\theta \rightarrow 0$ or $\theta \rightarrow 1$, since $\bar{P}_d \approx 0$ when $\theta \rightarrow 0$, and $\gamma_{th}(\theta) \rightarrow \infty$ when $\theta \rightarrow 1$. This indicates that there exists a θ which can maximize the D2D-Tx offloading radius.

VI. SIMULATION AND NUMERICAL RESULTS

In this section, we provide simulation results to evaluate the energy efficiency of the WPDO network. The network operates at $B = 10\text{MHz}$, $\lambda_B = 1 \times 10^{-5}\text{BSs/m}^2$, $\lambda_U = 1.5 \times 10^{-3}\text{UEs/m}^2$, $\lambda_D = 4 \times 10^{-4}\text{D2D-Txs/m}^2$, $P_m = 24\text{dBm}$, $N_t = 128$, $v_1 = 1\text{m}$, $v_2 = 5\text{m}$, $\alpha = 3$, $\beta = 2.5$, $\sigma^2 = 1 \times 10^{-11}\text{W}$, $\eta = 1$, $\varepsilon = 0.3$, unless otherwise stated.

In Fig.2, the average transmit power at a typical D2D-Tx is shown versus the density of D2D-Txs, where $\theta = 0.5$. We observe that the average transmit power at a typical D2D-Tx reduces with increasing the density of D2D-Txs, since the BS needs to wirelessly power more D2D-Txs in a certain communication time slot T while the total energy is limited. In addition, the average transmit power at a typical D2D-Tx increases with the BS antenna array size N_t as the radiated energy can be concentrated in a narrower beam and directly point the target D2D-Tx for WPT. Besides, the analytical results derived in this paper are validated by the Monte Carlo (MC) simulations.

In Fig.3, the expected minimum transmit power at a typical BS given in (18) is expressed regarding to the cellular UE data rate requirement R_c . Note that the BS expected minimum transmit power increases with the density of cellular UEs and the data rate requirement. When the density of cellular UEs increases, the allocated communication resources for

Algorithm 1 Energy efficiency of WPDO network.

Input:

- The network parameters, $\lambda_B, \lambda_D, \lambda_U, \alpha, \beta, B, \mathbb{P}_{con}, \eta, P_m, N_t, H_\alpha, H_\beta$;
- The required service data rates of cellular UEs and D2D UEs, R_c, R_d ;
- The maximum acceptable outage probability of D2D UE, ε ;
- The step length, ϖ .

Output:

- The near-optimal time allocation factor for WPT, θ^* ;
 - The maximum WPDO network energy efficiency, η_{EE}^* .
- 1: Initializing θ with ϖ ;
 - 2: Calculating the average transmit power at D2D-Tx \bar{P}_d based on (13) for a given value of θ ;
 - 3: Based on θ and \bar{P}_d , quantifying \mathcal{R}_D according to the equation of (29);
 - 4: Obtaining the WPDO network energy efficiency η_{EE} by combining equation (16), (18), (23) and (25-28);
 - 5: **for** $0 < \theta < 1$ **do**
 - 6: $\theta_n = \theta_{n-1} + \varpi$;
 - 7: $\theta = \theta_n$, repeating steps 2, 3, 4 and obtaining η'_{EE} ;
 - 8: **if** $\eta'_{EE} > \eta_{EE}$ **then**
 - 9: Substituting the value of η'_{EE} into η_{EE} ;
 - 10: **else**
 - 11: The near-optimal value of θ is θ_{n-1} , $\theta^* = \theta_{n-1}$;
 - 12: The maximum WPDO network energy efficiency is $\eta_{EE}^* = \eta_{EE}$.
 - 13: **Break**;
 - 14: **end if**
 - 15: **end for**
 - 16: **return** The near-optimal time allocation factor, θ^* ;
 - The maximum WPDO network energy efficiency, η_{EE}^* .

each cellular UE will be reduced. Therefore, to guarantee the cellular UE's required data rate, BS needs to provide more power to compensate for the lessened allocated bandwidth.

In Fig.4, the outage probability of a typical D2D UE given in (23) is presented against the time allocation factor θ . We observe that the outage probability of a typical D2D UE can be minimized by adjusting the parameter θ . This is because of the fact that, for a small value of θ , increasing θ improves the average transmit power at D2D-Tx and thus enhances the D2D information transmission. However, after the optimal θ for D2D outage probability, increasing θ decreases the time allocated for the D2D information transmission, and the

$$\begin{aligned} & \ln(1-\varepsilon) + \frac{2\lambda_D \pi^2}{\alpha \sin\left(\frac{2\pi}{\alpha}\right) H_\alpha^{\frac{2}{\alpha}}} \left(2^{\frac{R_d}{(1-\theta)B}} - 1\right)^{\frac{2}{\alpha}} \mathcal{R}_D^2 + \frac{\left(2^{\frac{R_d}{(1-\theta)B}} - 1\right) \sigma^2}{P_d H_\alpha} \mathcal{R}_D^\alpha \\ &= -\frac{2\lambda_B \left\{ \exp\left\{ \left[2^{\frac{R_c}{(1-\theta)B}} - 1\right] \frac{e^{-\mathbb{P}_{con} \pi \lambda_D \mathcal{R}_D^2 \lambda_U}}{\lambda_B} \right\} - 1 \right\}^{\frac{2}{\alpha}} \pi^2 \mathcal{R}_D^2}{\alpha \sin\left(\frac{2\pi}{\alpha}\right) N_t^{\frac{2}{\alpha}} \left(2^{\frac{R_d}{(1-\theta)B}} - 1\right)^{-\frac{2}{\alpha}} (P_d H_\alpha)^{\frac{2}{\alpha}}} \left\{ \left[\frac{\pi \lambda_D \bar{P}_d H_\alpha \alpha}{v_2^{\alpha-2} (\alpha-2)} + \sigma^2 \right] \frac{\Gamma\left(\frac{\alpha}{2} + 1\right)}{(\pi \lambda_B)^{\frac{\alpha}{2}}} + \frac{2P_m H_\alpha}{\alpha-2} \right\}^{\frac{2}{\alpha}}. \end{aligned} \quad (29)$$

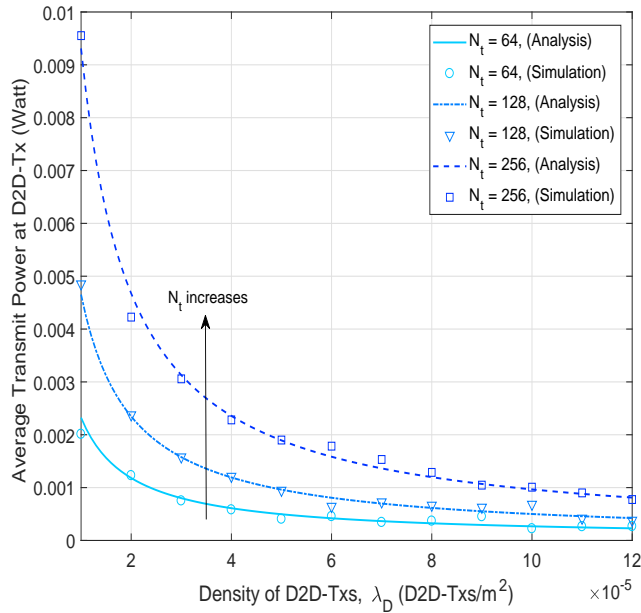


Fig 2: The average transmit power at D2D-Tx $\overline{P_d}$ given in (13) against the density of D2D-Txs λ_D under various BS antenna array size N_t .

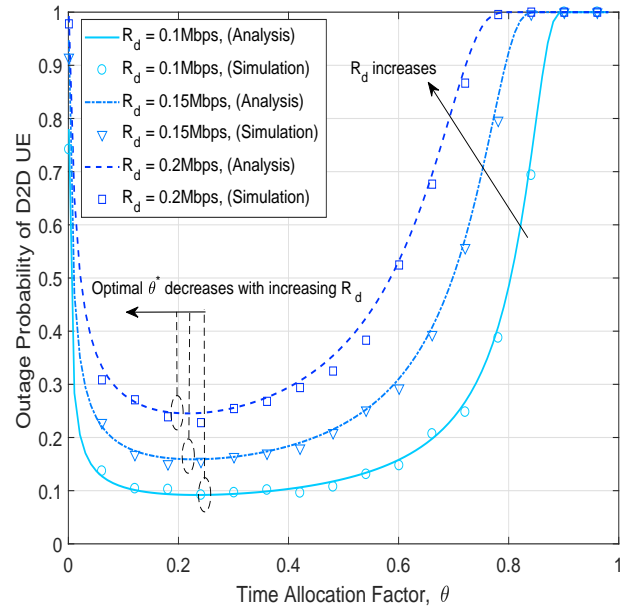


Fig 4: Outage probability of a typical D2D UE P_d^{out} given in (23) against the time allocation factor θ under various D2D UE data rate requirements R_d , where $\mathcal{R}_D = 50m$, $\lambda_U = 1 \times 10^{-3}$ UEs/m².

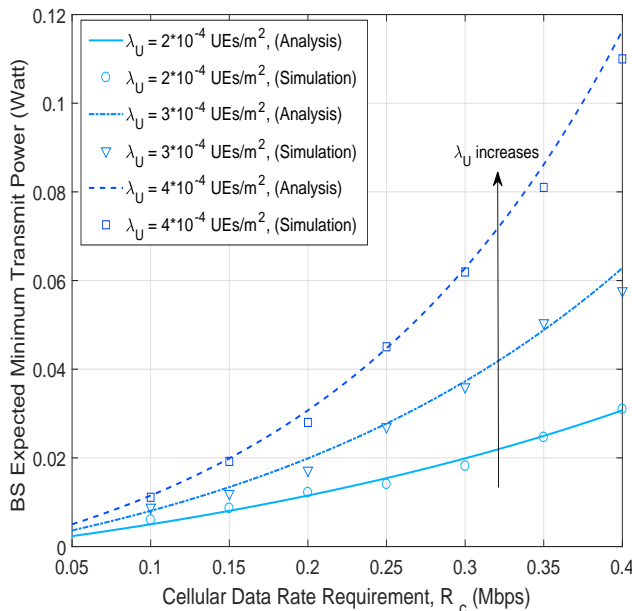


Fig 3: BS expected minimum transmit power given in (18) regarding to the cellular UE data rate requirement R_c under various densities of UEs λ_U , where $\theta = 0.5$.

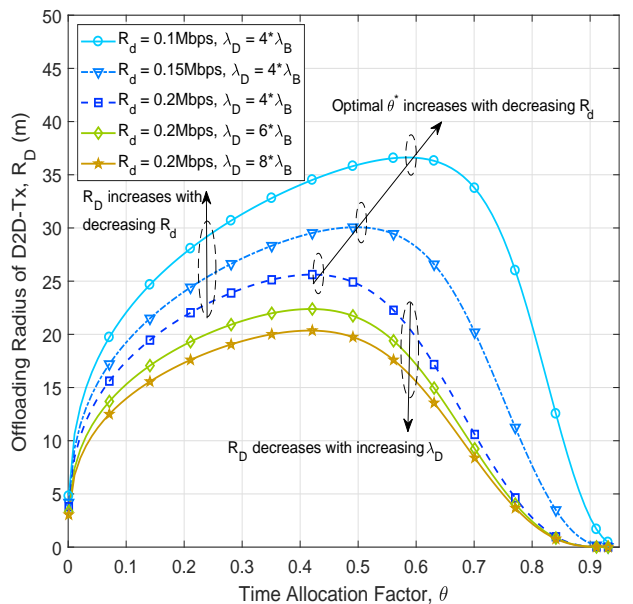


Fig 5: Offloading radius \mathcal{R}_D of a typical D2D-Tx given $\varepsilon = 0.3$ against the time allocation factor θ under different D2D UE data rate requirements R_d and D2D-Txs densities.

aggregated interference power goes up due to the higher average transmit power at D2D-Txs, which dramatically degrades the communication performance. Simulations are conducted to verify our theoretical results. The minor mismatches are resulted from that, in the theoretical results, the aggregated interference power is calculated in an infinite region, while in the simulations it is evaluated in a finite region, which results in the minor difference of the outage probability. Furthermore, another interesting observation can be found that, when D2D UE data rate requirement R_d gets large, it is desirable to divert larger fraction of time in a communication time slot

to the information transmission at D2D-Tx in order to lower the outage probability of D2D UE, while a larger fraction of time needs to be portioned for the WPT when R_d is small.

In Fig.5, we compare the offloading radius of a typical D2D-Tx against the time allocation factor θ , where the maximum acceptable outage probability ε is 0.3. The theoretical results are obtained according to the equation (29). We see that there exists a maximum offloading radius by selecting an appropriate θ , where the offloaded traffic in the WPDO network is maximized at this point. This is because of the fact that, when

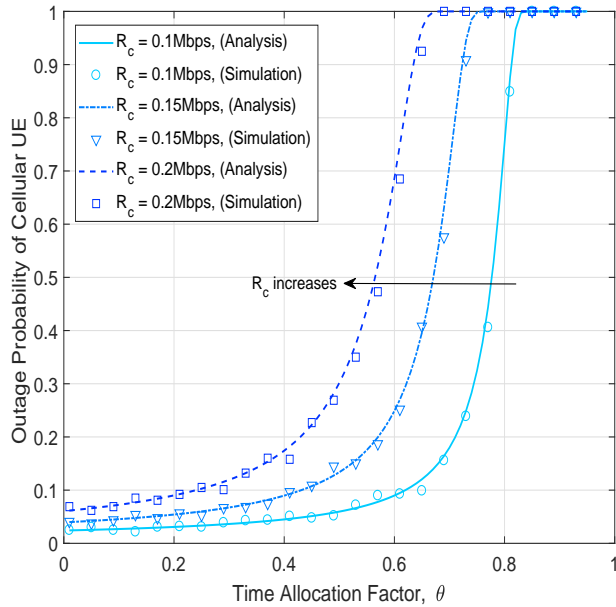


Fig 6: Outage probability of a typical cellular UE P_c^{out} given in (25) against the time allocation factor θ under various cellular UE data rate requirements R_c , where $R_d = R_c$.

θ is small, increasing θ results in a higher average transmit power at D2D-Tx and thus increases the offloading radius \mathcal{R}_D . However, when θ becomes large, the time allocated for D2D information transmission is reduced. Therefore, in this case, the link distance of D2D communications should be shrunken to guarantee the D2D UE data rate requirement R_d . In Fig.5, we also note that the offloading radius \mathcal{R}_D decreases with the data rate requirement R_d , which is in line with the intuition. In addition, the offloading radius \mathcal{R}_D decreases with the density of D2D-Txs, since the average transmit power is reduced at a D2D-Tx in accordance with Fig.2.

In Fig.6, the outage probability of a typical cellular UE given in (25) is shown against the time allocation factor θ . We observe that the outage probability of a typical cellular UE increases with the time allocation factor θ . This is because of the fact that increasing θ increases the aggregated interference power from D2D-Txs and reduces the time of BS information transmission, which degrades the performance of cellular link and thus improves the outage probability of a cellular UE. Further, we also see that the outage probability of a typical cellular UE increases with the cellular UE data rate requirements, and it approaches to 1 when θ becomes large.

Fig.7 depicts the WPDO network energy efficiency η_{EE} versus θ for different values of content popularity \mathbb{P}_{con} . As can be seen from Fig.7, the maximum WPDO network energy efficiency (η_{EE}^*) is obtained by optimizing the parameter θ . Specifically, when θ is small, the offloaded traffic is substantially rare which leads to the low energy efficiency. However, when θ gets large, the total energy consumption rises up due to the increased energy for WPT and the increased transmit power for BS information transmission, which results in a low network energy efficiency. Furthermore, it is interesting to see that the network energy efficiency is improved when the shared contents become more popular. In addition, the optimal

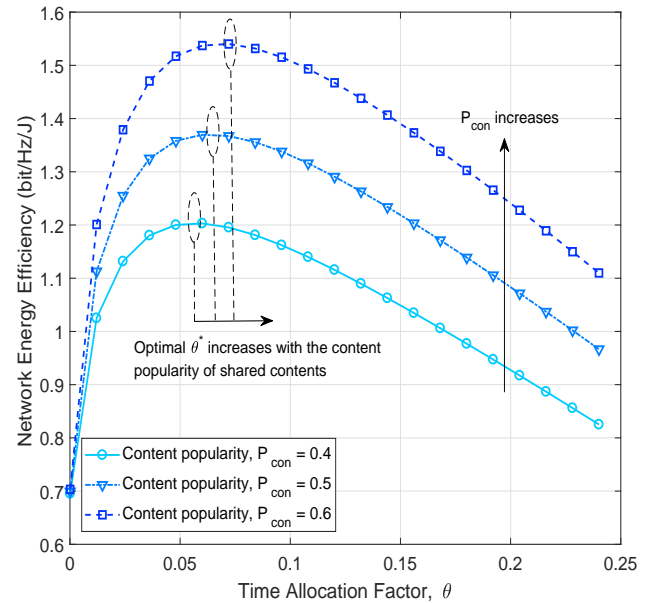


Fig 7: Network energy efficiency η_{EE} given in (26) against the time allocation factor θ for diverse content popularities \mathbb{P}_{con} , where $R_d = R_c = 0.2Mbps$.

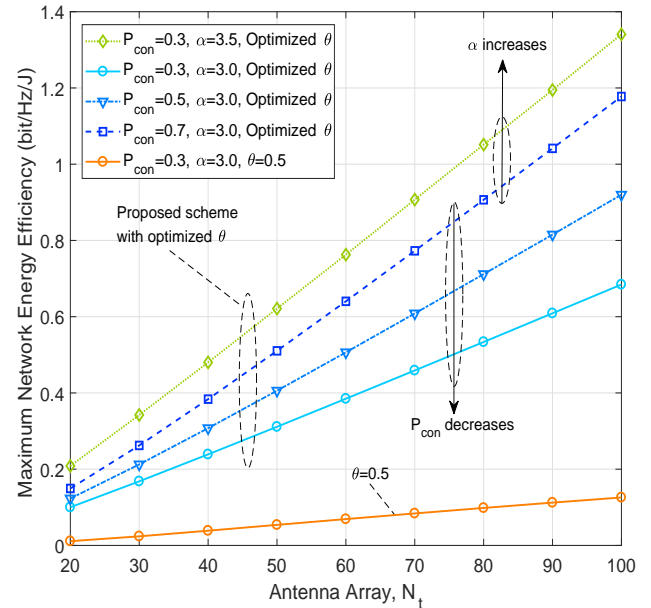


Fig 8: Maximum network energy efficiency η_{EE}^* against the BS antenna array size N_t for diverse content popularities \mathbb{P}_{con} and path loss exponent α , where $R_d = R_c = 0.2Mbps$.

time allocation factor θ^* increases with the content popularity \mathbb{P}_{con} of the shared contents. This indicates that the BSs should allocate more time fraction for WPT during a communication time slot to acquire a higher average transmit power at D2D-Txs as well as a larger offloading radius when the shared contents become popular.

In Fig.8, the maximum WPDO network energy efficiency (η_{EE}^*) is compared against the BS antenna array size N_t . We observe that η_{EE}^* increases with the number of elements in BS antenna arrays N_t . This suggests that the performance of the WPDO network is greatly improved by using the

massive antenna array size at each BS. In addition, Fig.8 shows that the WPDO network with larger path loss exponent of information transmission has better performance in terms of the network energy efficiency. Intuitively, co-tier and cross-tier interferences attenuate faster with a larger path loss exponent, which motivates the deployment of massive antenna arrays at BSs especially in the network with higher path loss. The results in Fig.8 also illustrate that η_{EE}^* increases with the content popularity \mathbb{P}_{con} , since more traffic can be offloaded to D2D links, which is a cost-effective way and improves the network capacity. In addition, in Fig.8, we also compare the proposed scheme, i.e., energy efficient WPDO network, with the case that the time allocation factor is fixed at 0.5. The results demonstrate that our proposed scheme achieves better performance in terms of the network energy efficiency.

VII. CONCLUSIONS

In this paper, we have modeled and analyzed wireless-powered D2D-assisted offloading (WPDO) in cellular networks. Considering the interference between cellular downlinks and underlaid D2D links and using stochastic geometry, we have derived the closed-form expressions of the average transmit power at D2D-Tx, the BS expected minimum transmit power, the D2D outage probability, and the cellular downlink outage probability. Based on the above analytical results, we have proposed an algorithm to maximize the WPDO network energy efficiency by optimizing the time allocation factor for WPT. The analytical and simulation results demonstrate that the WPT time allocation factor can be optimized to minimize the D2D outage probability and to maximize the WPDO network energy efficiency as well as the D2D offloading region. In addition, the WPDO network energy efficiency can be dramatically improved by using massive antenna arrays at BSs and by caching highly popular contents at D2D-Txs for content sharing. We have also provided useful insights into the design of an energy efficient WPDO network from a system-level perspective.

ACKNOWLEDGMENT

The authors appreciate the detailed feedback from the anonymous reviewers that have helped improve this paper substantially.

APPENDIX A PROOF OF PROPOSITION 1

According to (5), (6), (7) and (8), we have

$$\begin{aligned} \overline{P_d} &= \eta \frac{1}{(1-\theta)T} \mathbb{E} \left\{ E_{d_{k,j}}^{r,\theta T} \right\} \\ &= \frac{\eta\theta}{(1-\theta)n_d} \\ &\quad \cdot \left[\mathbb{E} \left\{ P_{d_{k,j}}^{r,\frac{1}{n_d}\theta T} \right\} + (n_d - 1) \mathbb{E} \left\{ P_{d_{k,j}}^{r,\frac{n_d-1}{n_d}\theta T} \right\} \right], \end{aligned} \quad (32)$$

where

$$\mathbb{E} \left\{ P_{d_{k,j}}^{r,\frac{1}{n_d}\theta T} \right\} = \mathbb{E} \left\{ P_{S_{b_j}}^{r,\frac{1}{n_d}\theta T} \right\} + \mathbb{E} \left\{ P_{S_{\Phi_B \setminus b_j}}^{r,\frac{1}{n_d}\theta T} \right\}. \quad (33)$$

Based on (5), the average received power $P_{S_{b_j}}^{r,\frac{1}{n_d}\theta T}$ from the nearest BS b_j by pointing beam is given by

$$\begin{aligned} &\mathbb{E} \left\{ P_{S_{b_j}}^{r,\frac{1}{n_d}\theta T} \right\} \\ &= \mathbb{E} \left\{ P_m \|\mathbf{h}_{b_j d_{k,j}}\|^2 H_\beta (\max\{\|b_j - d_{k,j}\|, v_1\})^{-\beta} \right\} \\ &\stackrel{(a)}{=} P_m N_t H_\beta \left[\int_0^{v_1} v_1^{-\beta} f_{\|b_j - d_{k,j}\|}(x) dx \right. \\ &\quad \left. + \int_{v_1}^\infty x^{-\beta} f_{\|b_j - d_{k,j}\|}(x) dx \right] \\ &\stackrel{(b)}{=} \frac{P_m N_t H_\beta v_1^{-\beta}}{(1 - e^{-\pi\lambda_B v_1^2})^{-1}} + \frac{P_m N_t H_\beta}{(\pi\lambda_B)^{-\frac{\beta}{2}}} \Gamma \left(1 - \frac{\beta}{2}, \pi\lambda_B v_1^2 \right) \end{aligned} \quad (34)$$

and

$$f_{\|b_j - d_{k,j}\|}(x) = 2\pi\lambda_B x e^{-\pi\lambda_B x^2} \quad (x > 0) \quad (35)$$

where $f_{\|b_j - d_{k,j}\|}(x)$ is the probability density function (PDF) of the distance $\|b_j - d_{k,j}\|$ [39], and (a) in (34) is obtained by using $\mathbb{E} \left\{ \|\mathbf{h}_{b_j d_{k,j}}\|^2 \right\} = N_t$ [32]. In step (b), $\Gamma(\cdot, \cdot)$ is the incomplete Gamma function.

In addition, the average received power $P_{S_{\Phi_B \setminus b_j}}^{r,\frac{1}{n_d}\theta T}$ from other BSs during $\frac{\theta T}{n_d}$ is calculated by, which is the second term of the right hand of the equation (33),

$$\begin{aligned} &\mathbb{E} \left\{ P_{S_{\Phi_B \setminus b_j}}^{r,\frac{1}{n_d}\theta T} \right\} \\ &= \sum_{b_n \in \Phi_B \setminus b_j} \mathbb{E} \left\{ P_m \left| \mathbf{h}_{b_n d_{k,j}} \frac{\mathbf{g}_{b_n d_{l,n}}^H}{\|\mathbf{g}_{b_n d_{l,n}}\|} \right|^2 H_\beta \right\} \\ &\quad \cdot \mathbb{E} \left\{ (\max\{\|b_n - d_{l,n}\|, v_1\})^{-\beta} \right\} \\ &\stackrel{(a)}{=} P_m H_\beta \mathbb{E}_{\Phi_B} \left\{ \sum_{b_n \in \Phi_B \setminus b_j} (\max\{\|b_n - d_{l,n}\|, v_1\})^{-\beta} \right\} \\ &= P_m H_\beta 2\pi\lambda_B \int_{\|b_j - d_{k,j}\|}^\infty r (\max\{r, v_1\})^{-\beta} dr \\ &= P_m H_\beta 2\pi\lambda_B \left[\int_0^\infty f_{\|b_j - d_{k,j}\|}(x) \int_x^\infty r^{1-\beta} dr dx \right. \\ &\quad \cdot \mathbb{P}\{x > v_1\} + \left. \left(\int_0^\infty f_{\|b_j - d_{k,j}\|}(x) \int_x^{v_1} v_1^{-\beta} r dr dx \right. \right. \\ &\quad \left. \left. + \int_{v_1}^\infty r^{1-\beta} dr \right) \mathbb{P}\{x \leq v_1\} \right] \\ &= P_m H_\beta 2\pi\lambda_B \left[\frac{\Gamma\left(2 - \frac{\beta}{2}\right)}{\beta - 2} (\pi\lambda_B)^{\frac{\beta}{2}-1} e^{-\pi\lambda_B v_1^2} \right. \\ &\quad \left. + \left(\frac{1}{2} v_1^{2-\beta} - \frac{1}{2} v_1^{-\beta} \frac{1}{\pi\lambda_B} + \frac{v_1^{2-\beta}}{\beta - 2} \right) \left(1 - e^{-\pi\lambda_B v_1^2} \right) \right] \end{aligned} \quad (36)$$

where (a) follows from $\left| \mathbf{h}_{b_n d_{k,j}} \frac{\mathbf{g}_{b_n d_{l,n}}^H}{\|\mathbf{g}_{b_n d_{l,n}}\|} \right|^2 \sim \exp(1)$, $\Gamma(\cdot)$ is the standard Gamma function, and more specifically we have

$$\mathbb{P}\{x > v_1\} = \int_{v_1}^\infty f_{\|b_j - d_{k,j}\|}(x) dx = e^{-\pi\lambda_B v_1^2}, \quad (37)$$

$$\mathbb{P}\{x \leq v_1\} = 1 - \mathbb{P}\{x > v_1\} \quad (38)$$

where $f_{\|b_j - d_{k,j}\|}(x)$ is given in (35).

Based on (6), the average received power $P_{d_{k,j}}^{r, \frac{n_d-1}{n_d}\theta T}$ at $d_{k,j}$ during $\frac{(n_d-1)\theta T}{n_d}$ is given by

$$\begin{aligned} & \mathbb{E}\left\{P_{d_{k,j}}^{r, \frac{n_d-1}{n_d}\theta T}\right\} \\ &= \sum_{b_n \in \Phi_B, d_{l,j} \neq d_{k,j}} \mathbb{E}\left\{\left|\mathbf{h}_{b_n d_{k,j}} \frac{\mathbf{g}_{b_n d_{l,n}}^H}{\|\mathbf{g}_{b_n d_{l,n}}\|}\right|^2\right\} \\ & \cdot P_m H_\beta \mathbb{E}\left\{(\max\{\|b_n - d_{l,n}\|, v_1\})^{-\beta}\right\} \\ &= P_m H_\beta \mathbb{E}_{\Phi_B} \left\{ \sum_{b_n \in \Phi_B \setminus b_j} (\max\{\|b_n - d_{l,n}\|, v_1\})^{-\beta} \right\} \\ &= P_m H_\beta 2\pi\lambda_B \int_0^\infty r (\max\{r, v_1\})^{-\beta} dr \\ &= P_m H_\beta 2\pi\lambda_B v_1^{-\beta} \frac{1}{2} v_1^2 + P_m H_\beta 2\pi\lambda_B \frac{v_1^{2-\beta}}{\beta-2} \\ &= P_m H_\beta \pi\lambda_B v_1^{2-\beta} \left(1 + \frac{2}{\beta-2}\right). \end{aligned} \quad (39)$$

Combining (33), (34), (36) and (39) into (32) and with some mathematical manipulation, we have the desired result in (13).

APPENDIX B PROOF OF PROPOSITION 2

Given a typical cellular UE $u_{i,j}^c$ which requests data rate R_c during the communication time slot T , the expected minimum transmit power at its serving BS b_j during the subslot $(1-\theta)T$ is given by a transformation of (1) as follows

$$\begin{aligned} & \mathbb{E}_I \left\{ P_{i,j}^B | N_j^c, \|b_j - u_{i,j}^c\| \right\} \\ &= \frac{2^{\frac{R_c N_j^c}{(1-\theta)B}} - 1}{\|b_j - u_{i,j}^c\|^{-\alpha} N_t} \mathbb{E} \left\{ I_{u_{i,j}^c}^C + I_{u_{i,j}^c}^D + \sigma^2 \right\}, \end{aligned} \quad (40)$$

where $\mathbb{E}_I[x]$ denotes taking expectation of variable x on the interference power I , and we have utilized $\mathbb{E}\left\{\left\|\mathbf{h}_{b_j u_{i,j}^c}\right\|^2\right\} = N_t$, which characterizes the average performance in channel.

We consider the worst-case scenario, where the interfering BSs transmit at the maximum allowable transmit power, and thus we have

$$\begin{aligned} & \mathbb{E} \left\{ I_{u_{i,j}^c}^C | y_{i,j}^c = \|b_n - u_{i,j}^c\| \right\} \\ & \leq \mathbb{E}_{h, \Phi_B} \left\{ \sum_{b_n \in \Phi_B \setminus b_j} \left| \mathbf{h}_{b_n u_{i,j}^c} \frac{\mathbf{g}_{b_n u_{i,n}^c}^H}{\|\mathbf{g}_{b_n u_{i,n}^c}\|} \right|^2 \frac{P_m H_\alpha}{\|b_n - u_{i,j}^c\|^\alpha} \right\} \\ & \stackrel{(a)}{=} \frac{P_m H_\alpha}{(2\pi\lambda_B)^{-1}} \int_{y_{i,j}^c}^\infty x^{1-\alpha} dx \\ &= \frac{2\pi\lambda_B P_m H_\alpha}{(\alpha-2)(y_{i,j}^c)^{\alpha-2}}, \end{aligned} \quad (41)$$

where (a) is obtained by using Campbell's Theorem, and we have utilized $\mathbb{E}\left\{\left|\mathbf{h}_{b_n u_{i,j}^c} \frac{\mathbf{g}_{b_n u_{i,n}^c}^H}{\|\mathbf{g}_{b_n u_{i,n}^c}\|}\right|^2\right\} = 1$. $y_{i,j}^c =$

$\|b_j - u_{i,j}^c\|$ is the distance between $u_{i,j}^c$ and its associated BS. In addition, we have

$$\begin{aligned} & \mathbb{E} \left\{ I_{u_{i,j}^c}^D \right\} \\ &= \mathbb{E}_{h, \Phi_D} \left\{ \sum_{d_{l,n} \in \Phi_D} \frac{\overline{P_d} h_{d_{k,j} u_{i,j}^c} H_\alpha}{(\max\{\|d_{l,n} - u_{i,j}^c\|, v_2\})^\alpha} \right\} \\ & \stackrel{(a)}{=} 2\pi\lambda_D \overline{P_d} H_\alpha \left(\int_0^{v_2} v_2^{-\alpha} x dx + \int_{v_2}^\infty x^{-\alpha} x dx \right) \\ &= \overline{P_d} H_\alpha \pi\lambda_D v_2^{2-\alpha} \left(1 + \frac{2}{\alpha-2}\right), \end{aligned} \quad (42)$$

where (a) follows from $h_{d_{k,j} u_{i,j}^c} \sim \exp(1)$.

Combining (41) and (42) into (40), we obtain the upper bound expression of $\mathbb{E}\{P_{i,j}^B | N_j^c, y_{i,j}^c\}$ as follows

$$\begin{aligned} & \mathbb{E} \left\{ P_{i,j}^B | N_j^c, y_{i,j}^c \right\} \\ & \leq \frac{2^{\frac{N_j^c R_c}{(1-\theta)B}} - 1}{(y_{i,j}^c)^{-\alpha} N_t} \left[\frac{2\pi\lambda_B P_m H_\alpha}{(\alpha-2)(y_{i,j}^c)^{\alpha-2}} + \frac{\pi\lambda_D \overline{P_d} H_\alpha \alpha}{v_2^{\alpha-2}(\alpha-2)} + \sigma^2 \right]. \end{aligned} \quad (43)$$

Considering that the PDF of $y_{i,j}^c$ is $f_{y_{i,j}^c}(y) = 2\pi\lambda_B y e^{-\pi\lambda_B y^2}$ ($y > 0$), we decondition the variable $y_{i,j}^c$ in $\mathbb{E}\{P_{i,j}^B | N_j^c, y_{i,j}^c\}$ and obtain the approximate $\mathbb{E}\{P_{i,j}^B | N_j^c\}$ as follows

$$\begin{aligned} & \mathbb{E} \left\{ P_{i,j}^B | N_j^c \right\} \\ & \approx \int_0^\infty \mathbb{E} \left\{ P_{i,j}^B | N_j^c, y_{i,j}^c \right\} f_{y_{i,j}^c}(y) dy \\ &= \frac{\left(2^{\frac{N_j^c R_c}{(1-\theta)B}} - 1\right) 2\pi\lambda_B}{(\alpha-2) N_t} \left\{ \left[\frac{\pi\lambda_D \overline{P_d} H_\alpha \alpha}{v_2^{\alpha-2}} + (\alpha-2)\sigma^2 \right] \right. \\ & \left. \cdot \int_0^\infty y^{\alpha+1} e^{-\pi\lambda_B y^2} dy + 2\pi\lambda_B P_m H_\alpha \int_0^\infty y^3 e^{-\pi\lambda_B y^2} dy \right\}. \end{aligned} \quad (44)$$

By calculating (44), we have the result in (15), which completes the proof.

APPENDIX C PROOF OF PROPOSITION 4

According to (21) and (9), we have

$$\begin{aligned} & \mathbb{E} \left\{ P_d^{out} | \mathcal{R}_D, I_{u_{i,k,j}^d}^C, I_{u_{i,k,j}^d}^D \right\} \\ &= 1 - \Pr \left\{ \frac{\overline{P_d} h_{d_{k,j} u_{i,k,j}^d} H_\alpha \mathcal{R}_D^{-\alpha}}{I_{u_{i,k,j}^d}^C + I_{u_{i,k,j}^d}^D + \sigma^2} \geq \gamma_{th}(\theta) \right\} \\ &= 1 - \Pr \left\{ h_{d_{k,j} u_{i,k,j}^d} \geq \psi(\theta, R_d) \left(I_{u_{i,k,j}^d}^C + I_{u_{i,k,j}^d}^D + \sigma^2 \right) \right\} \\ & \stackrel{(a)}{=} 1 - e^{-\psi(\theta, R_d)\sigma^2} \mathcal{L}_{I_{u_{i,k,j}^d}^C} \left\{ \psi(\theta, R_d) \right\} \mathcal{L}_{I_{u_{i,k,j}^d}^D} \left\{ \psi(\theta, R_d) \right\} \end{aligned} \quad (45)$$

where $\psi(\theta, R_d) = \frac{\gamma_{th}(\theta)}{P_d H_\alpha \mathcal{R}_D^{-\alpha}}$ is given in (23), (a) follows from $h_{d_{k,j} u_{i,k,j}^d} \sim \exp(1)$, $\mathcal{L}_{I_{u_{i,k,j}^d}^C}\{\cdot\}$ and $\mathcal{L}_{I_{u_{i,k,j}^d}^D}\{\cdot\}$ denotes the Laplace transform of $I_{u_{i,k,j}^d}^C$ and $I_{u_{i,k,j}^d}^D$, respectively.

In addition, we have

$$\begin{aligned} & \mathcal{L}_{I_{u_{i,k,j}^d}^C}\{s\} \\ &= \mathbb{E} \left\{ \exp \left(-s \sum_{b_n \in \Phi_B} P_{i,n}^B \right. \right. \\ & \quad \cdot \left. \left. \left| \mathbf{h}_{b_n u_{i,k,j}^d} \frac{\mathbf{g}_{b_n u_{i,k,j}^d}^H}{\|\mathbf{g}_{b_n u_{i,k,j}^d}\|} \right|^2 H_\alpha \|b_n - u_{i,k,j}^d\|^{-\alpha} \right) \right\} \\ &= \mathbb{E}_{\Phi_B} \left\{ \prod_{b_n \in \Phi_B} \frac{1}{1 + s P_{i,n}^B H_\alpha \|b_n - u_{i,k,j}^d\|^{-\alpha}} \right\} \\ &\stackrel{(a)}{\approx} \exp \left\{ -2\pi \lambda_B \int_0^\infty \left(1 - \frac{1}{1 + s \mathbb{E}\{P_j^B\} H_\alpha x^{-\alpha}} \right) x dx \right\} \\ &= \exp \left\{ -\frac{2\lambda_B (\mathbb{E}\{P_j^B\})^{\frac{2}{\alpha}} \pi^2}{\alpha \sin\left(\frac{2\pi}{\alpha}\right)} s^{\frac{2}{\alpha}} \right\} \end{aligned} \quad (46)$$

where in (a) we have utilized $\mathbb{E}\{P_j^B\}$ given in (18) to denote the interfering power from cellular BSs.

Furthermore, $\mathcal{L}_{I_{u_{i,k,j}^d}^D}\{s\}$ is given by

$$\begin{aligned} & \mathcal{L}_{I_{u_{i,k,j}^d}^D}\{s\} \\ &= \mathbb{E} \left\{ \exp \left(-s \sum_{d_n \in \Phi_D \setminus d_{k,j}} \frac{\bar{P}_d h_{d_n u_{i,k,j}^d} H_\alpha}{\|d_n - u_{i,k,j}^d\|^\alpha} \right) \right\} \\ &= \mathbb{E} \left\{ \exp \left(-s \sum_{d_n \in \Phi_D^{B(o, l_{i,k,j}^d)}, d_n \neq d_k} \frac{\bar{P}_d h_{d_n u_{i,k,j}^d} H_\alpha}{\|d_n - u_{i,k,j}^d\|^\alpha} \right. \right. \\ & \quad \left. \left. - s \sum_{d_n \in \Phi_D^{\bar{B}(o, l_{i,k,j}^d)}, d_n \neq d_k} \frac{\bar{P}_d h_{d_n u_{i,k,j}^d} H_\alpha}{\|d_n - u_{i,k,j}^d\|^\alpha} \right) \right\} \\ &\approx \exp \left\{ -2\pi \lambda_D \int_0^{l_{i,k,j}^d} \left(1 - \frac{1}{1 + s \bar{P}_d H_\alpha x^{-\alpha}} \right) x dx \right\} \\ & \cdot \exp \left\{ -2\pi \lambda_D \int_{l_{i,k,j}^d}^\infty \left(1 - \frac{1}{1 + s \bar{P}_d H_\alpha x^{-\alpha}} \right) x dx \right\} \\ &= \exp \left\{ -\frac{2\lambda_D (\bar{P}_d)^{\frac{2}{\alpha}} \pi^2}{\alpha \sin\left(\frac{2\pi}{\alpha}\right)} s^{\frac{2}{\alpha}} \right\} \end{aligned} \quad (47)$$

where $\Phi_D^{B(o, l_{i,k,j}^d)}$ is the set of D2D-Txs that are located in $B(o, l_{i,k,j}^d)$ which is a circular region centered at the origin with radius $l_{i,k,j}^d$, and $l_{i,k,j}^d$ is the distance between the D2D UE $u_{i,k,j}^d$ and its connecting D2D-Tx $d_{k,j}$ in j^{th} cell. Besides, $\Phi_D^{\bar{B}(o, l_{i,k,j}^d)}$ is the set of D2D-Txs that are located outside

the region of $B(o, l_{i,k,j}^d)$. In (47), we approximate that the set of interfering D2D-Txs follows a PPP distribution with density λ_D and then utilize the probability generating function to calculate the Laplace transform of $I_{u_{i,k,j}^d}^D$.

Combining (46) and (47) into (45), we have

$$\begin{aligned} P_d^{out} &= 1 - \exp \left\{ -\frac{2 \left[\lambda_B (\mathbb{E}\{P_j^B\})^{\frac{2}{\alpha}} + \lambda_D (\bar{P}_d)^{\frac{2}{\alpha}} \right] \pi^2}{\alpha \sin\left(\frac{2\pi}{\alpha}\right)} \right. \\ & \quad \cdot \left. \left(\frac{\gamma_{th}(\theta)}{P_d H_\alpha \mathcal{R}_D^{-\alpha}} \right)^{\frac{2}{\alpha}} - \frac{\gamma_{th}(\theta)}{P_d H_\alpha \mathcal{R}_D^{-\alpha}} \sigma^2 \right\} \end{aligned} \quad (48)$$

where \bar{P}_d and $\mathbb{E}\{P_j^B\}$ are given in (13) and (18), respectively, which completes the proof.

APPENDIX D PROOF OF PROPOSITION 5

According to (24), the outage probability of a typical cellular UE conditioned on the link distance $y_{i,j}^c$, channel power gain $\|\mathbf{h}_{b_j u_{i,j}^c}\|^2$ and the number of cellular UEs N_j^c in its cell is obtained as follows

$$\begin{aligned} & \mathbb{E} \left\{ P_c^{out} | y_{i,j}^c, \|\mathbf{h}_{b_j u_{i,j}^c}\|^2, N_j^c \right\} \\ &= 1 - \mathbb{P} \left\{ P_{i,j}^B(R_c) \leq P_m | y_{i,j}^c, \|\mathbf{h}_{b_j u_{i,j}^c}\|^2 \right\} \\ &= 1 - \mathbb{P} \left\{ I_{u_{i,j}^c}^{agg} \leq \frac{P_m \|\mathbf{h}_{b_j u_{i,j}^c}\|^2}{\left(2^{\frac{R_c N_j^c}{(1-\theta)B}} - 1 \right) (y_{i,j}^c)^\alpha} - \sigma^2 \right\} \quad (49) \\ &= 1 - F_{I_{u_{i,j}^c}^{agg}} \left(\frac{P_m \|\mathbf{h}_{b_j u_{i,j}^c}\|^2}{\left(2^{\frac{R_c N_j^c}{(1-\theta)B}} - 1 \right) (y_{i,j}^c)^\alpha} - \sigma^2 \right) \end{aligned}$$

where $F_{I_{u_{i,j}^c}^{agg}}(x)$ is the Cumulative Distribution Function (CDF) of $I_{u_{i,j}^c}^{agg}$, and $I_{u_{i,j}^c}^{agg} = I_{u_{i,j}^c}^C + I_{u_{i,j}^c}^D$ denotes the aggregated interference power from cellular and D2D links at $u_{i,j}^c$.

In addition, we have

$$\mathcal{L}_{I_{u_{i,j}^c}^{agg}}\{s\} = \mathbb{E} \left\{ \exp(-s I_{u_{i,j}^c}^{agg}) \right\} = \int_0^\infty e^{-st} f_{I_{u_{i,j}^c}^{agg}}(t) dt, \quad (50)$$

and

$$f_{I_{u_{i,j}^c}^{agg}}(t) = \mathcal{L}^{-1} \left\{ \mathcal{L}_{I_{u_{i,j}^c}^{agg}}\{s\} \right\} \quad (51)$$

where $f_{I_{u_{i,j}^c}^{agg}}(t)$ denotes the PDF of $I_{u_{i,j}^c}^{agg}$ and $\mathcal{L}^{-1}(\cdot)$ represents the inverse Laplace transform.

Based on the properties of Laplace transform, $\mathcal{L}_{I_{u_{i,j}^c}^{agg}}\{s\}$ can be expressed as

$$\mathcal{L}_{I_{u_{i,j}^c}^{agg}}\{s\} = \mathcal{L}_{I_{u_{i,j}^c}^C}\{s\} \mathcal{L}_{I_{u_{i,j}^c}^D}\{s\} \quad (52)$$

where $\mathcal{L}_{I_{u_{i,j}^c}^C}\{s\}$ denotes the Laplace transform of the aggregated interference power from cellular BSs, while $\mathcal{L}_{I_{u_{i,j}^c}^D}\{s\}$

is the Laplace transform of the aggregated interference power from D2D-Txs. More specifically, we can obtain

$$\begin{aligned} \mathcal{L}_{I_{u_{i,j}^c}} \{s\} &= \mathbb{E} \left\{ \exp \left(-s \sum_{b_n \in \Phi_B \setminus b_j} H_\alpha P_{i,n}^B \right. \right. \\ &\quad \cdot \left. \left. \left| \frac{\mathbf{h}_{b_n u_{i,j}^c}}{\|\mathbf{h}_{b_n u_{i,j}^c}\|} \right|^2 \left\| b_n - u_{i,j}^c \right\|^{-\alpha} \right) \right\} \quad (53) \\ &\approx \exp \left\{ -\pi \lambda_B \zeta \left(s, y_{i,j}^c, P_m \right) \right\} \end{aligned}$$

where

$$\begin{aligned} \zeta \left(s, y_{i,j}^c, P_m \right) &= \frac{2sP_m \left(y_{i,j}^c \right)^{2-\alpha}}{\alpha - 2} \\ &\quad \cdot {}_2F_1 \left[1, 1 - \frac{2}{\alpha}; 2 - \frac{2}{\alpha}; -\frac{sP_m}{\left(y_{i,j}^c \right)^\alpha} \right] \quad (54) \end{aligned}$$

where $y_{i,j}^c = \|b_j - u_{i,j}^c\|$ is the distance between the typical cellular UE $u_{i,j}^c$ and its nearest BS b_j , and ${}_2F_1[a, b; c; d]$ is the Gauss Hypergeometric function.

The Laplace transform of $I_{u_{i,j}^D}^D$ is given by

$$\begin{aligned} \mathcal{L}_{I_{u_{i,j}^D}} \{s\} &= \mathbb{E} \left\{ \exp \left(-s \sum_{d_n \in \Phi_D} \frac{\overline{P_d} h_{d_n u_{i,j}^D} H_\alpha}{\|d_n - u_{i,j}^D\|^\alpha} \right) \right\} \quad (55) \\ &= \exp \left\{ -\frac{2\lambda_D \left(\overline{P_d} \right)^{\frac{2}{\alpha}} \pi^2}{\alpha \sin \left(\frac{2\pi}{\alpha} \right)} s^{\frac{2}{\alpha}} \right\} \end{aligned}$$

where $\overline{P_d}$ is given in (13).

Therefore, the Laplace transform of $I_{u_{i,j}^c}^{agg}$ is obtained as follows

$$\mathcal{L}_{I_{u_{i,j}^c}^{agg}} \{s\} = \exp \left\{ - \left[\pi \lambda_B \zeta \left(s, y_{i,j}^c, P_m \right) + \xi s^{\frac{2}{\alpha}} \right] \right\} \quad (56)$$

where $\xi = \frac{2\lambda_D \left(\overline{P_d} \right)^{\frac{2}{\alpha}} \pi^2}{\alpha \sin \left(\frac{2\pi}{\alpha} \right)}$ being same with the expression in (25).

According to (51), we obtain the CDF of $I_{u_{i,j}^c}^{agg}$ as

$$\begin{aligned} F_{I_{u_{i,j}^c}^{agg}}(x) &= \mathbb{P} \left(I_{u_{i,j}^c}^{agg} \leq x \right) \\ &= \int_0^x f_{I_{u_{i,j}^c}^{agg}}(t) dt \\ &= \int_0^x \frac{1}{2\pi i} \lim_{T \rightarrow \infty} \int_{c-iT}^{c+iT} e^{st} \mathcal{L}_{I_{u_{i,j}^c}^{agg}}(s) ds dt \\ &= \frac{1}{2\pi i} \lim_{T \rightarrow \infty} \int_{c-iT}^{c+iT} \left(\frac{e^{sx} - 1}{s} \right) \mathcal{L}_{I_{u_{i,j}^c}^{agg}} \{s\} ds \\ &= \frac{1}{2\pi i} \lim_{T \rightarrow \infty} \int_{c-iT}^{c+iT} \frac{e^{sx - \pi \lambda_B \zeta \left(s, y_{i,j}^c, P_m \right) - \xi s^{\frac{2}{\alpha}}}}{s} ds. \quad (57) \end{aligned}$$

Considering equation (57) has a branch point at the origin, we use the Bromwich inversion method with a specified

contour to calculate the integral [40] as follows

$$\begin{aligned} F_{I_{u_{i,j}^c}^{agg}}(x) &= - \lim_{R \rightarrow \infty} \frac{1}{2\pi i} \left\{ \int_{-\pi}^{-\pi} e^{re^{i\theta} x - \pi \lambda_B \zeta \left(re^{i\theta}, y_{i,j}^c, P_m \right) - \xi r^{\frac{2}{\alpha}} e^{\frac{2i\theta}{\alpha}}} \right. \\ &\quad \cdot id\theta + \int_R^r e^{ue^{i\pi} x - \pi \lambda_B \zeta \left(ue^{i\pi}, y_{i,j}^c, P_m \right) - \xi u^{\frac{2}{\alpha}} e^{\frac{2i\pi}{\alpha}}} \frac{du}{u} \\ &\quad \left. + \int_r^R e^{ue^{-i\pi} x - \pi \lambda_B \zeta \left(ue^{-i\pi}, y_{i,j}^c, P_m \right) - \xi u^{\frac{2}{\alpha}} e^{-\frac{2i\pi}{\alpha}}} \frac{du}{u} \right\} \\ &= - \lim_{R \rightarrow \infty} \frac{1}{2\pi i} \left\{ -2\pi i + \int_R^r e^{-ux - \pi \lambda_B \zeta \left(-u, y_{i,j}^c, P_m \right)} \right. \\ &\quad \cdot \left(e^{-\xi u^{\frac{2}{\alpha}} \left[\cos \left(\frac{2\pi}{\alpha} \right) + i \sin \left(\frac{2\pi}{\alpha} \right) \right]} \right. \\ &\quad \left. \left. - e^{-\xi u^{\frac{2}{\alpha}} \left[\cos \left(\frac{2\pi}{\alpha} \right) - i \sin \left(\frac{2\pi}{\alpha} \right) \right]} \right) \frac{du}{u} \right\} \\ &= - \lim_{R \rightarrow \infty} \frac{1}{2\pi i} \left\{ -2\pi i + \int_R^r e^{-ux - \pi \lambda_B \zeta \left(-u, y_{i,j}^c, P_m \right)} \right. \\ &\quad \cdot e^{-\xi u^{\frac{2}{\alpha}} \cos \left(\frac{2\pi}{\alpha} \right)} \left(e^{-\xi u^{\frac{2}{\alpha}} i \sin \left(\frac{2\pi}{\alpha} \right)} - e^{\xi u^{\frac{2}{\alpha}} i \sin \left(\frac{2\pi}{\alpha} \right)} \right) \frac{du}{u} \left. \right\} \\ &= 1 - \frac{1}{\pi} \int_0^\infty e^{-ux - \pi \lambda_B \zeta \left(-u, y_{i,j}^c, P_m \right) - \xi u^{\frac{2}{\alpha}} \cos \left(\frac{2\pi}{\alpha} \right)} \\ &\quad \cdot \sin \left(\xi u^{\frac{2}{\alpha}} \sin \left(\frac{2\pi}{\alpha} \right) \right) \frac{du}{u} \\ &= 1 - \frac{\alpha}{2\pi} \int_0^\infty e^{-\left(\frac{t}{\xi}\right)^{\frac{\alpha}{2}} x} e^{-\pi \lambda_B \zeta \left(-\left(\frac{t}{\xi}\right)^{\frac{\alpha}{2}}, y_{i,j}^c, P_m \right)} \\ &\quad \cdot e^{-t \cos \left(\frac{2\pi}{\alpha} \right)} \sin \left(t \sin \left(\frac{2\pi}{\alpha} \right) \right) \frac{dt}{t} \quad (58) \end{aligned}$$

where in the last step we have utilized $t = \xi u^{\frac{2}{\alpha}}$.

Now we are in the position of computing the outage probability of a typical cellular UE as follows

$$\begin{aligned} \mathbb{E} \{ P_c^{out} | N_j^c \} &= \int_0^\infty \int_0^\infty \mathbb{E} \left\{ P_c^{out} | y_{i,j}^c, \left\| \mathbf{h}_{b_j u_{i,j}^c} \right\|^2, N_j^c \right\} \\ &\quad \cdot f_{\left\| \mathbf{h}_{b_j u_{i,j}^c} \right\|^2} (h) f_{y_{i,j}^c} (y) dh dy \\ &= 1 - \int_0^\infty \int_0^\infty F_{I_{u_{i,j}^c}^{agg}} \left(\left(2^{\frac{R_c N_j^c}{(1-\theta)B}} - 1 \right) P_m h y^{-\alpha} - \sigma^2 \right) \\ &\quad \cdot f_{\left\| \mathbf{h}_{b_j u_{i,j}^c} \right\|^2} (h) f_{y_{i,j}^c} (y) dh dy \\ &= \frac{\alpha \lambda_B \Gamma \left(\frac{N_t}{2} \right)}{\Gamma(N_t)} \int_0^\infty \int_0^\infty \sin \left(t \sin \left(\frac{2\pi}{\alpha} \right) \right) y \\ &\quad \cdot \frac{\left(t^{\frac{\alpha}{2}} y^{-\alpha} \xi^{-\frac{\alpha}{2}} P_m \left(2^{\frac{R_c N_j^c}{(1-\theta)B}} - 1 \right)^{-1} + 1 \right)^{-\frac{N_t}{2}}}{\pi \lambda_B \zeta \left(-t^{\frac{\alpha}{2}} \xi^{-\frac{\alpha}{2}}, y, P_m \right) + \frac{t}{\sin \left(\frac{2\pi}{\alpha} \right)} - \sigma^2 t^{\frac{\alpha}{2}} \xi^{-\frac{\alpha}{2}} + \pi \lambda_B y^2} dt dy \quad (59) \end{aligned}$$

where $f_{\left\| \mathbf{h}_{b_j u_{i,j}^c} \right\|^2} (h)$ is the PDF of $\left\| \mathbf{h}_{b_j u_{i,j}^c} \right\|^2$ which follows from the Gamma distribution as

$$f_{\left\| \mathbf{h}_{b_j u_{i,j}^c} \right\|^2} (h) = \frac{1}{\Gamma(N_t)} h^{N_t-1} e^{-h}. \quad (60)$$

Finally, we have the desired result by calculating the following summation of series

$$P_c^{out} = \sum_{n=1}^{\infty} \mathbb{E} \{ P_c^{out} | N_j^c \} g_{N_j^c}(n) \quad (61)$$

which completes the proof.

REFERENCES

- [1] B. Shang, L. Zhao, K. C. Chen, and X. Chu, "Energy efficient D2D-assisted offloading with wireless power transfer," in *GLOBECOM 2017 - 2017 IEEE Global Communications Conference*, Dec 2017, pp. 1–6.
- [2] A. Asadi, Q. Wang, and V. Mancuso, "A survey on device-to-device communication in cellular networks," *IEEE Communications Surveys Tutorials*, vol. 16, no. 4, pp. 1801–1819, Fourthquarter 2014.
- [3] H. Chen, L. Xiao, D. Yang, T. Zhang, and L. Cuthbert, "User cooperation in wireless powered communication networks with a pricing mechanism," *IEEE Access*, vol. 5, pp. 16 895–16 903, 2017.
- [4] S. Bi, C. K. Ho, and R. Zhang, "Wireless powered communication: Opportunities and challenges," *IEEE Communications Magazine*, vol. 53, no. 4, pp. 117–125, April 2015.
- [5] Y. Zeng, B. Clerckx, and R. Zhang, "Communications and signals design for wireless power transmission," *IEEE Transactions on Communications*, vol. PP, no. 99, pp. 1–1, 2017.
- [6] R. Zhang and C. K. Ho, "MIMO broadcasting for simultaneous wireless information and power transfer," *IEEE Transactions on Wireless Communications*, vol. 12, no. 5, pp. 1989–2001, May 2013.
- [7] M. M. Mowla, I. Ahmad, D. Habibi, and Q. V. Phung, "A green communication model for 5G systems," *IEEE Transactions on Green Communications and Networking*, vol. 1, no. 3, pp. 264–280, Sept 2017.
- [8] S. Singh and J. G. Andrews, "Joint resource partitioning and offloading in heterogeneous cellular networks," *IEEE Transactions on Wireless Communications*, vol. 13, no. 2, pp. 888–901, February 2014.
- [9] Y. He, M. Chen, B. Ge, and M. Guizani, "On WiFi offloading in heterogeneous networks: Various incentives and trade-off strategies," *IEEE Communications Surveys Tutorials*, vol. 18, no. 4, pp. 2345–2385, Fourthquarter 2016.
- [10] J. Jiang, S. Zhang, B. Li, and B. Li, "Maximized cellular traffic offloading via device-to-device content sharing," *IEEE Journal on Selected Areas in Communications*, vol. 34, no. 1, pp. 82–91, Jan 2016.
- [11] Y. Shen, C. Jiang, T. Q. S. Quek, and Y. Ren, "Device-to-device-assisted communications in cellular networks: An energy efficient approach in downlink video sharing scenario," *IEEE Transactions on Wireless Communications*, vol. 15, no. 2, pp. 1575–1587, Feb 2016.
- [12] Y. Cao, T. Jiang, X. Chen, and J. Zhang, "Social-aware video multicast based on device-to-device communications," *IEEE Transactions on Mobile Computing*, vol. 15, no. 6, pp. 1528–1539, June 2016.
- [13] M. Ding, P. Wang, D. Lopez-Perez, G. Mao, and Z. Lin, "Performance impact of LoS and NLoS transmissions in dense cellular networks," *IEEE Transactions on Wireless Communications*, vol. 15, no. 3, pp. 2365–2380, March 2016.
- [14] S. Lee and K. Huang, "Coverage and economy of cellular networks with many base stations," *IEEE Communications Letters*, vol. 16, no. 7, pp. 1038–1040, July 2012.
- [15] H. A. Omar, K. Abboud, N. Cheng, K. R. Malekshan, A. T. Gamage, and W. Zhuang, "A survey on high efficiency wireless local area networks: Next generation WiFi," *IEEE Communications Surveys Tutorials*, vol. 18, no. 4, pp. 2315–2344, Fourthquarter 2016.
- [16] B. Shang, L. Zhao, K. C. Chen, and X. Chu, "An economic aspect of device-to-device assisted offloading in cellular networks," *IEEE Transactions on Wireless Communications*, vol. 17, no. 4, pp. 2289–2304, April 2018.
- [17] Y. Guo, L. Duan, and R. Zhang, "Optimal pricing and load sharing for energy saving with cooperative communications," *IEEE Transactions on Wireless Communications*, vol. 15, no. 2, pp. 951–964, Feb 2016.
- [18] L. Wang, H. Wu, W. Wang, and K. C. Chen, "Socially enabled wireless networks: Resource allocation via bipartite graph matching," *IEEE Communications Magazine*, vol. 53, no. 10, pp. 128–135, October 2015.
- [19] P. Grover and A. Sahai, "Shannon meets Tesla: Wireless information and power transfer," in *2010 IEEE International Symposium on Information Theory*, June 2010, pp. 2363–2367.
- [20] K. Huang and V. K. N. Lau, "Enabling wireless power transfer in cellular networks: Architecture, modeling and deployment," *IEEE Transactions on Wireless Communications*, vol. 13, no. 2, pp. 902–912, February 2014.
- [21] H. Ju and R. Zhang, "Throughput maximization in wireless powered communication networks," *IEEE Transactions on Wireless Communications*, vol. 13, no. 1, pp. 418–428, January 2014.
- [22] H. H. Yang, J. Lee, and T. Q. S. Quek, "Heterogeneous cellular network with energy harvesting-based D2D communication," *IEEE Transactions on Wireless Communications*, vol. 15, no. 2, pp. 1406–1419, Feb 2016.
- [23] A. H. Sakr and E. Hossain, "Cognitive and energy harvesting-based D2D communication in cellular networks: Stochastic geometry modeling and analysis," *IEEE Transactions on Communications*, vol. 63, no. 5, pp. 1867–1880, May 2015.
- [24] S. Gupta, R. Zhang, and L. Hanzo, "Energy harvesting aided device-to-device communication underlying the cellular downlink," *IEEE Access*, vol. PP, no. 99, pp. 1–1, 2016.
- [25] K. Huang and X. Zhou, "Cutting the last wires for mobile communications by microwave power transfer," *IEEE Communications Magazine*, vol. 53, no. 6, pp. 86–93, June 2015.
- [26] H. Wang, J. Wang, G. Ding, L. Wang, T. A. Tsiftsis, and P. K. Sharma, "Resource allocation for energy harvesting-powered D2D communication underlying UAV-assisted networks," *IEEE Transactions on Green Communications and Networking*, vol. PP, no. 99, pp. 1–1, 2017.
- [27] M. L. Ku and J. W. Lai, "Joint beamforming and resource allocation for wireless-powered device-to-device communications in cellular networks," *IEEE Transactions on Wireless Communications*, vol. 16, no. 11, pp. 7290–7304, Nov 2017.
- [28] Y. Zhu, L. Wang, K. K. Wong, S. Jin, and Z. Zheng, "Wireless power transfer in massive mimo-aided hetnets with user association," *IEEE Transactions on Communications*, vol. 64, no. 10, pp. 4181–4195, Oct 2016.
- [29] Y. Li, M. Qian, D. Jin, P. Hui, Z. Wang, and S. Chen, "Multiple mobile data offloading through disruption tolerant networks," *IEEE Transactions on Mobile Computing*, vol. 13, no. 7, pp. 1579–1596, July 2014.
- [30] M. Chen, W. Saad, C. Yin, and M. Debbah, "Echo state networks for proactive caching in cloud-based radio access networks with mobile users," *IEEE Transactions on Wireless Communications*, vol. 16, no. 6, pp. 3520–3535, June 2017.
- [31] A. Damnjanovic, J. Montojo, J. Cho, H. Ji, J. Yang, and P. Zong, "UE's role in LTE advanced heterogeneous networks," *IEEE Communications Magazine*, vol. 50, no. 2, pp. 164–176, February 2012.
- [32] Y. Deng, L. Wang, M. ElKashlan, M. D. Renzo, and J. Yuan, "Modeling and analysis of wireless power transfer in heterogeneous cellular networks," *IEEE Transactions on Communications*, vol. 64, no. 12, pp. 5290–5303, Dec 2016.
- [33] H. Q. Ngo, M. Matthaiou, T. Q. Duong, and E. G. Larsson, "Uplink performance analysis of multicell MU-SIMO systems with ZF receivers," *IEEE Transactions on Vehicular Technology*, vol. 62, no. 9, pp. 4471–4483, Nov 2013.
- [34] I. Krikidis, S. Sasaki, S. Timotheou, and Z. Ding, "A low complexity antenna switching for joint wireless information and energy transfer in mimo relay channels," *IEEE Transactions on Communications*, vol. 62, no. 5, pp. 1577–1587, May 2014.
- [35] K. Huang, "Spatial throughput of mobile ad hoc networks powered by energy harvesting," *IEEE Transactions on Information Theory*, vol. 59, no. 11, pp. 7597–7612, Nov 2013.
- [36] O. Ozel, J. Yang, and S. Ulukus, "Optimal broadcast scheduling for an energy harvesting rechargeable transmitter with a finite capacity battery," *IEEE Transactions on Wireless Communications*, vol. 11, no. 6, pp. 2193–2203, June 2012.
- [37] X. Zhou, R. Zhang, and C. K. Ho, "Wireless information and power transfer: Architecture design and rate-energy tradeoff," in *2012 IEEE Global Communications Conference (GLOBECOM)*, Dec 2012, pp. 3982–3987.
- [38] S. Singh, H. S. Dhillon, and J. G. Andrews, "Offloading in heterogeneous networks: Modeling, analysis, and design insights," *IEEE Transactions on Wireless Communications*, vol. 12, no. 5, pp. 2484–2497, May 2013.
- [39] M. Haenggi, *Stochastic Geometry for Wireless Networks*. Cambridge University Press, 2012.
- [40] A. M. Cohen, *Numerical Methods for Laplace Transform Inversion*. Springer Publishing Company, Incorporated, 2007.